PSI-1177/
TR-1305

ULTRAVIOLET EMISSIONS OCCURRING ABOUT HYPERSONIC VEHICLES IN RAREFIED FLOWS

Final Report

George E. Caledonia and Robert H. Krech
Physical Sciences Inc.
20 New England Business Center
Andover, MA 01810

April 1994

U.S. Army Research Office

Contract No. DAAH04-93-C-0015

Dr. David Mann
U.S. Army Research Office
4300 S. Miami Boulevard
Research Triangle Park, NC 27709-2211

Approved for Public Release

Distribution Unlimited

REPORT DOCUMENTATION PAGE

Form Approved
OMB No. 0704-0188

1. AGENCY USE ONLY *(Leave blank)*	2. REPORT DATE	3. REPORT TYPE AND DATES COVERED
	April 1994	Final - 4 Jun 93 - 4 Feb 94

4. TITLE AND SUBTITLE

Ultraviolet Emissions Occurring about Hypersonic Vehicles in Rarefied Flows

5. FUNDING NUMBERS

DAAH04-93-C-0015

6. AUTHOR(S)

George E. Caledonia and R.H. Krech

7. PERFORMING ORGANIZATION NAME(S) AND ADDRESS(ES)

Physical Sciences Inc.
20 New England Business Center
Andover, MA 01810-1077

8. PERFORMING ORGANIZATION REPORT NUMBER

PSI-1177/TR-1305

9. SPONSORING/MONITORING AGENCY NAME(S) AND ADDRESS(ES)

U.S. Army Research Office
P.O. Box 12211
Research Triangle Park, NC 27709-2211

10. SPONSORING/MONITORING AGENCY REPORT NUMBER

ARO 31210.2-EG-SDI

11. SUPPLEMENTARY NOTES

12a. DISTRIBUTION/AVAILABILITY STATEMENT

The views, opinions and/or findings contained in this report are those of the author(s) and should not be construed as official Department of the Army position, policy, or decision, unless so designated by other documentation.

12b. DISTRIBUTION CODE

13. ABSTRACT ***(Maximum 200 words)***

This report includes: (1) an investigation of the kinetic mechanisms for the visible shuttle glow; (2) an overview of flight and laboratory investigations of VUV to IR surface glows observed at hypersonic velocities in low earth orbit conditions; (3) a summary of the flight-measured absolute intensities observed for rarefied ram flow at VUV, UV and visible wavelengths as a function of altitude; and (4) a brief look at seeker sensor survivability/ viability issues associated with a High Velocity Missile (HVM) intended for boost phase interception.

14. SUBJECT TERMS			15. NUMBER OF PAGES
			16. PRICE CODE
17. SECURITY CLASSIFICATION OF REPORT	18. SECURITY CLASSIFICATION OF THIS PAGE	19. SECURITY CLASSIFICATION OF ABSTRACT	20. LIMITATION OF ABSTRACT
Unclassified	Unclassified	Unclassified	UL

Memorandum of Transmittal

U.S. Army Research Office
Atten: SLCRO-IP-Library
P.O. Box 12211
Research Triangle Park, NC 27709-2211

Dear Library Technician:

- ☐ Reprint (15 copies)
- ☐ Technical Report (50 copies)
- ☐ Manuscript (1 copy)
- ☒ Final Report (50 copies)
- ☐ Thesis (1 copy)
  - ☐ MS
  - ☐ PhD
  - ☐ Other _____

Title: Ultraviolet Emissions Occurring About Hypersonic Vehicles in Rarefied Flows (PSI-1177/TR-1305)

is forwarded for your information.

SUBMITTED FOR PUBLICATION TO (applicable only if report is manuscript):

_____

_____

Sincerely,

George E. Caledonia

George E. Caledonia 31210-EG-SDI
President
Physical Sciences Inc.
20 New England Business Center
Andover, MA 01810

TABLE OF CONTENTS

LIST OF FIGURES

SUMMARY

This effort was primarily directed towards addressing phenomenology of surface catalyzed glows which can occur in the low-earth orbit environment and which were relevant to the Skipper mission. The study included:

1. The development of a detailed kinetic model for the visible glow
2. Experimental evaluation of key kinetic parameters of the model
3. A survey and review of previous glow measurements and evaluations
4. An examination of radiative mechanisms important to high velocity interceptor missiles.

The key technical participants were Messrs. George E. Caledonia and Robert H. Krech. A presentation is planned for the Fall 1994 AGU Meeting and a journal article is in preparation. No inventions were developed during the course of this effort.

1. INTRODUCTION

Activities have been varied during the subject program. A detailed review of low earth orbit surface glow measurements was prepared and presented at the annual Missile Signatures Group meeting at NASA Ames Research Center on 29 April 1993. This review covered flight and laboratory observations of glows over the spectral region from the vacuum ultraviolet to the infrared. A copy of the viewgraphs presented at that meeting is included as Appendix A.

A major effort was the development of a general kinetic model for the visible glow coupled with an analytical and experimental assessment of the various required kinetic parameters. This work is described in Section 2.

Also, we have re-examined the glow data base to provide a summary of the flight-measured absolute glow intensities observed in the VUV, UV and visible. For ease of use these measurements were converted to a geometry corresponding to a view from the surface into the ram direction. This brief review, which should be of use in setting optical instrument gains for the rarefied flow portion of the Skipper Mission , is presented in Section 3.

Lastly, we have provided a brief study of issues relevant to the sensor survivability/ capability of a High Velocity Missile (HVM) to be used for theater missile defense. Preliminary thoughts are provided in Section 4. Bremsstrahlung radiation has been identified as an important shock front emission feature for anticipated HVM operating conditions. A brief overview of this radiation phenomena is provided in Section 4.

2. KINETIC MODEL FOR THE VISIBLE SHUTTLE GLOWS

2.1 Introduction

Surface glows have been observed above ram surfaces of both space shuttle and satellites operating in low-earth orbit (LEO). The most prominent of these, observed in both the visible[1-3] and the infrared,[4] is apparently due to surface catalyzed recombination of O and NO. A second glow observed in the vacuum ultraviolet (VUV)[5] appears to result from surface catalyzed recombination of nitrogen atoms.[6-8] In this work we will review the kinetics appropriate to surface glow formation in general and develop a detailed model for the visible glow.

The next section provides an exposition of the kinetics relevant to the visible glow and an evaluation of the glow dependencies on atmosphere densities and kinetic parameters. This is followed by a description of laboratory experimental activities directed towards evaluating key kinetic parameters. Lastly, these new results are reviewed in the light of the proposed kinetic mechanism so as to ascertain our present understanding of the visible glow.

2.2 Glow Kinetic Model

Surface catalyzed reactions are generally considered in two limits. The first of these is the Langmuir-Hinshelwood mechanism, where the assumption is made that both species accommodate to the surface before recombining. The second is the Rideal mechanism, where it is assumed that one species accommodates to the surface and then reacts with a second species impinging upon the surface. These are two limiting cases, since depending on collision angle and velocity, different levels of surface accommodation can occur prior to reactions.

The Langmuir-Hinshelwood mechanism is generally preferred. Indeed, a Rideal mechanism has never been clearly identified. Nonetheless, Swenson and Meyerott[6] recently interpreted the LEO VUV glow in terms of a Rideal mechanism, apparently in order to obtain the observed altitude dependence of the glow intensity.

The visible shuttle glow is ascribed to the surface formation of NO_2^* in the low earth orbit (free molecular) environment. In this section we develop a model for the glow based upon a specific NO formation mechanism. We then write general relationships including all potentially important kinetic mechanisms and then specialize the results to more likely candidates. The general relationship is developed under the assumption that the Langmuir-Hinshelwood mechanism pertains, i.e., where surface adsorbed NO and O react to form electronically excited NO_2 which is released in the gas phase. A question remains as to the source of NO in this free molecular, essentially single collision, environment. One possibility is the reaction between incident and scattered ambient O and N_2, see Figure 1.

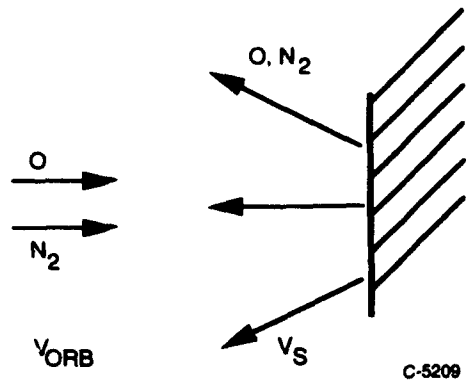

Figure 1. Scattering Geometry

The reaction

$$O + N_2 \overset{\sigma}{\sim} NO + N \qquad (1)$$

is endothermic for center of mass (COM) energies <3.26 eV. This, coincidentally, approximately corresponds to the COM energy of an O, N_2 pair interacting at the orbital velocity of 8 km/s. Thus interactions between incoming and scattered O/N_2, which will occur at velocities exceeding 8 km/s, can produce NO. Indeed the cross-section for producing vibrationally excited NO by this process has recently been evaluated as a function of O-atom velocity.[9]

Furthermore it is anticipated that the velocity of scattered species will be less than that of the incident species, with magnitude depending on the nature of the interaction. Therefore, the center of mass velocity of the interacting pair, and their products, will be directed towards the surface. Thus this reaction provides a clear source of surface NO for the glow reaction.

A simple model for the production rate of NO can be provided under the assumption of diffuse scattering, a likely scenario for rough surfaces. Given a characteristic spacecraft dimension R then the concentration of scattered species at a distance r from the surface is

$$N_s(r) = N_s(o) \left(\frac{R}{r+R}\right)^2 \frac{V_{ORB}}{V_s} \qquad (2)$$

where the velocity ratio accounts for the increase in density resulting from the lower velocity V_s of the scattered particles.

The total flux of NO produced is then given by

$$F_{NO} = 2 \int_o^\infty \sigma(V_{cm})\, V_{cm}\, N_o\, N_{N_2} \frac{V_{ORB}}{V_s} \left(\frac{R}{r+R}\right)^2 dr \qquad (3)$$

where we have neglected the differences in COM velocity between O and N_2 (the factor of 2 signifies that either $\vec{O}/\vec{N}_2$ or $\vec{N}_2/\vec{O}$ can occur). Whence

$$F_{NO} \approx 2\sigma \, V \, N_O \, N_{N_2} \, R \, \frac{V_{ORB}}{V_s} \tag{4}$$

To first order the center of mass velocity will be of order $V_{orbital}$. We will choose V_s = 1 km/s and $\sigma = 10^{-17}$ cm^2. At this time V_s is undefined, however if V_s is larger, then the cross section will be also[9] and thus this estimate for the ratio is reasonable.

$$F_{NO} \approx 2 \times 10^{-22} \, R \, F_O \, F_{N_2} \text{ cm}^{-2}\text{-s}^{-1} \tag{5}$$

2.3 Surface Coverage of NO and O

The surface coverage of NO and O which is the ultimate rate determining step in the production of the visible glow can be a complicated function of ambient density and concentration, surface temperature, material, etc. In this section we will write down the general contributing mechanisms and then simplify to tractable relationships which will exhibit potential visible glow intensity altitude dependencies. The model is appropriate to the free molecular flow limit.

2.3.1 The Phenomenology

The driving forces are the fluxes of species impacting the surface. These fluxes are the product of local number density and velocity and are in units of cm^{-2} s^{-1}. We will divide the fluxes into three categories: F_O, F_{NO} and F_X, where F_X is mean to represent the remaining atmospheric species, largely N_2. The relevant kinetics are summarized in Table 1.

The O and NO will exhibit a sticking efficiency S_O, S_{NO} upon impacting the surface. This efficiency will be temperature, velocity and material dependent.

Once the O and NO are upon the surface several effects can occur:

1. Thermal desorption, τ_O, τ_{NO} cm^{-2}-s. Temperature dependent

2. Collisional desorption, flux dependent. Since the NO is in small concentration only F_O and F_X are important and these have collisional desorption efficiencies designated C_O and C_X for NO and similarly C′ for O collisions. These are temperature, material and velocity dependent.

Table 1. Surface Kinetics for O + NO

Reaction Type	Process	Kinetic Quantity
Adsorption	$O(g) \xrightarrow{S_O} O(S)$ $NO(g) \xrightarrow{S_{NO}} NO(S)$	Sticking Coefficient
Thermal Desorption	$O(S) \xrightarrow{\tau_O^{-1}} O(g)$ $NO(S) \xrightarrow{\tau_{NO}^{-1}} NO(g)$	Thermal Desorption Rate
Collisional Desorption	$O(g) + O(S) \xrightarrow{C'_O} 2\,O(g)$ $\rightarrow O_2(g)$ $X(g) + O(S) \xrightarrow{C'_X} X(g) + O(g)$ $O(g) + NO(S) \xrightarrow{C_O} O(g) + NO(g)$ $\rightarrow NO_2(g)$ $X(g) + NO(S) \xrightarrow{C_X} X(g) + NO(g)$	Collisional Desorption Efficiency
Surface Reaction	$O(s) + NO(S) \xrightarrow{R_{NO_2}} NO_2(g)$ $O(s) + O(S) \xrightarrow{R_{O_2}} O_2(g)$	Reaction Rate

3. Chemical reaction on the surface, i.e.,

$$O(s) + NO(s) \rightarrow NO_2\ (g) \tag{6}$$

$$O(s) + O(s) \rightarrow O_2\ (g) \tag{7}$$

with rates designated R_{NO_2}, R_{O_2} which will be temperature and material dependent.

2.3.2 Master Equations

We will write the master equations in terms of surface coverage g where

$$1 = g_O + g_{NO} + g_{VOID}\ , \tag{8}$$

and we are assuming monolayer coverage, i.e., normalization factor is $\approx 3 \times 10^{15}$ cm^{-2} and that the O and NO surface cross sections are the same. In this notation

$$\begin{aligned} dg_{NO}/dt = {} & F_{NO}\, S_{NO}\, (1 - g_O - g_{NO})/N_S - g_{NO}/\tau_{NO} \\ & - (F_O\, C_O + F_X\, C_X)\, g_{NO}/N_S - g_{NO}\, g_O\, R_{NO_2} \end{aligned} \tag{9}$$

$$\begin{aligned} dg_O/dt = {} & F_O\, S_O\, (1 - g_O - g_{NO})/N_S - g_O/\tau_O \\ & - (F_O\, C_O' + F_X\, C_X')\, g_O/N_S - g_{NO}\, g_O\, R_{NO_2} - g_O^2\, R_{O_2} \end{aligned} \tag{10}$$

which have steady state solutions

$$g_{NO} = \frac{F_{NO}\, S_{NO}\, (1 - g_O)/N_S}{F_{NO}\, S_{NO}/N_S + \tau_{NO}^{-1} + F_O\, C_O/N_S + F_X\, C_X/N_S + g_O\, R_{NO_2}} \tag{11}$$

$$g_O = \frac{-B + \sqrt{B^2 + 4R_{O_2} F_O S_O (1 - g_{NO})/N_S}}{2R_{O_2}} \qquad (12)$$

where $B = F_O S_O/N_S + \tau_O^{-1} + F_O C_O'/N_S + F_X C_X'/N_S + g_{NO} R_{NO_2}$, and N_S is the surface coverage normalization factor of $\sim 3 \times 10^{15}$ cm^{-2}.

Note that we have assumed that O and NO compete for surface sites and that N_2 accommodation may be neglected. These assumptions need not be necessary or warranted as discussed later on in the text.

These relationships are sill uncoupled and relatively complex so that it is difficult to discern scaling laws. We will make a few simplifying assumptions to proceed further:

a) Assume the O is chemisorbed so that τ_O is very long

b) Neglect collisional desorption by species X. These are minor species at altitudes of interest

c) Assume $g_{NO} << g_O$

d) Neglect surface recombination of O-atoms

e) Assume NO_2 formation can never be a dominant loss mechanism.

Let us now consider the case where collisional desorption dominates the loss mechanisms for surface O and NO. In this limit, appropriate for lower altitudes

$$g_O = \frac{S_O}{C_O' + S_O} \qquad (13)$$

$$g_{NO} = \frac{F_{NO} S_{NO} C_O'/(C_O' + S_O)}{F_{NO} S_{NO} + F_O C_O} \quad . \qquad (14)$$

The flux of NO_2 produced, F_{NO_2}, is given by

$$F_{NO_2} = N_S R_{NO_2} g_{NO} g_O \quad . \qquad (15)$$

Since we anticipate that $F_O >> F_{NO}$, Eq. (15) reduces to

$$F_{NO_2} = N_S R_{NO_2} \frac{F_{NO}}{F_O} \frac{S_{NO} S_O C_O'}{C_O} \frac{1}{(C_O' + S_O)^2} \tag{16}$$

and substituting the expression for F_{NO}, Eq. (5), into Eq. (16) results in

$$F_{NO_2} = 2 \times 10^{-22} A R F_{N_2} \frac{S_O C_O'}{C_O} \frac{1}{(C_O' + S_O)^2} \tag{17}$$

or linear with N_2 density. Such scaling is in reasonable agreement with the AE data.[10]

Alternatively, Swenson et al.[11] have suggested that NO thermal desorption is responsible for the variation in the intensities of space shuttle glow observations. If NO thermal desorption is the dominant loss process then

$$g_{NO} = F_{NO} S_{NO} \frac{C_O'}{C_O' + S_O} \tau_{NO}/N_S \tag{18}$$

whence

$$F_{NO_2} = 2 \times 10^{-22} R F_O F_{N_2} \tau_{NO} \frac{S_{NO} S_O C_O'}{(C_O' + S_O)^2} \tag{19}$$

exhibiting a density squared dependence.

Of course, other density dependencies can be realized through various estimates of the unknown parameters in relationships (11) and (12).

The basic conclusion of this exercise is that there are sufficient undefined parameters to preclude an *a priori* definition of the dominant glow kinetic mechanisms and anticipated behavior.

In the next section we describe an experimental effort using our fast oxygen atom source which attempts to evaluate some of these kinetic parameters so as to provide a more definitive description of the glow.

2.4 Experimental Studies

Our concept is to study the kinetics of NO surface coverage using the intensity of the visible glow as a measure of NO surface concentration. Basically, a material, in this case clear anodized aluminum which was considered as a material of choice for the Skipper mission, is subjected under vacuum to a background concentration of NO. The material is then intermittently impinged by a pulse of 8 km/s oxygen atoms produced by PSI's fast oxygen atom source.[12-14] Since the fluence of O-atoms per pulse is constant, the relative glow intensity presumably provides a measure of the NO coverage.

Let us first consider a simple model for the NO surface coverage of a material initially in vacuum which is instantaneously subjected to a constant background pressure of NO. We limit our discussion to monolayer coverage since at the temperature of interest the NO vapor pressure is too high to produce a deeper surface layer of NO.

Let f be the fractional coverage of NO on the surface, S_{NO} be the sticking coefficient, and τ_{NO} be the characteristic time for thermal desorption. Then

$$\frac{df}{dt} = \frac{(NO)}{N_s}\frac{\bar{c}}{4} S_{NO} (1-f) - \frac{f}{\tau_{NO}} \tag{20}$$

where N_s is the previously defined monolayer surface coverage, (NO) is the local NO concentration in cm^{-3}, and $\bar{c}$ is the mean NO molecular speed.

This has the steady state solution

$$f_s = \frac{S_{NO}(NO)\bar{c}/4}{S_{NO}(NO)\bar{c}/4 + \tau_{NO}^{-1} N_s} \tag{21}$$

which can be recast as

$$\frac{f_s}{1-f_s} = \frac{S_{NO}(NO)}{N_s}(\bar{c}/4)\tau_{NO} \quad . \tag{22}$$

Thus, if one can measure f_s versus NO concentration, one could measure the product S_{NO} τ_{NO}. This is a straightforward steady-state measurement.

The time dependent solution of Eq. (1) provides additional information. This is

$$f = f_s\left(1 - e^{-\left(\frac{(NO)}{N_s}\frac{\bar{c}}{4}S_{NO} + \tau_{NO}^{-1}\right)t}\right) \quad . \tag{23}$$

Thus, by monitoring f at early times, after the NO flow is turned on, one can back out the overall characteristic time, whichever dominates.

If we now bombard this surface with a pulse of fast oxygen atoms, with pulse fluence much less than N_s (monolayer surface coverage), then the resulting integrated NO_2^* fluorescence is given by

$$I_{NO_2^*}\frac{Phot}{cm^2} = F_o f N_s \epsilon \tag{24}$$

where F_o is the O pulse line density and ϵ is the efficiency of producing NO_2^*. This "efficiency" is in units of cm^{-3} and has built into it the residence time of O-atoms on the surface.

Note here that this intensity must be integrated over both wavelength and sterradiancy. It should be noted that for the NO_2 continuum, over half this intensity will fall in the IR and thus visible measurements should be corrected accordingly.

If the sample temperature is varied, Eq. (24) can be used to evaluate the change in ϵ, if the surface is kept saturated. Note that as the temperature is varied, changes in ϵ will also reflect changes in the O-atom sticking coefficient and thermal desorption time as well as the change in the reaction efficiency. In the present effort we have only been able to investigate this behavior for room temperature samples.

In an earlier effort[15] we did examine collisional and thermal desorption of NO at liquid nitrogen temperatures. Then we deduced thermal desorption times of ~65s for materials such as aluminum and Z_3O_6. O-atom collisional desorption efficiencies were found to be ~4 to 8%. Our suspicion however, is that NO collisional desorption does not play an important role in the glow mechanism.

Our experimental measurements were performed on a target plate 15.2 cm high by 35.6 cm long. The plate was placed some 72.5 cm from the nozzle throat and was completely engulfed by the O-beam which was pulsed at 2 Hz. A typical O-beam fluence per pulse at the plate was 3.6×10^{14} cm^{-2}, a fraction of a monolayer. The plate temperature was held at 290 K.

The glow intensity was measured just above the plate at a central wavelength of 630 nm with a 10 nm bandpass. This wavelength is just to the blue of peak glow intensity. The optical field of view was cylindrical with a 3.2 cm diameter.

The O-beam exhibits a small intrinsic radiation level at this wavelength. Furthermore the beam interacts with the gaseous NO to produce a continuum glow. As previously discussed[13] this gas phase glow is blue-shifted related to the surface glow, and most likely results from energetic oxygen atom interactions with dimers.

The measurements of glow intensity above the surface will necessarily include a contribution from this gas phase glow as well as from the surface glow. These relative contributions are distinguished by performing the intensity measurements with and without the target in place. The difference in intensities between these two measurements is taken to be the contribution of the surface glow.

A typical glow signal observed during a pulse of the O-beam is shown in Figure 2 for an NO pressure of 10^{-4} Torr. The O-beam full width at half maximum is around 75 μs at this distance as reflected in the observed pulse shape. As can be seen the signal is much higher when the target plate is placed in the path of the O-beam.

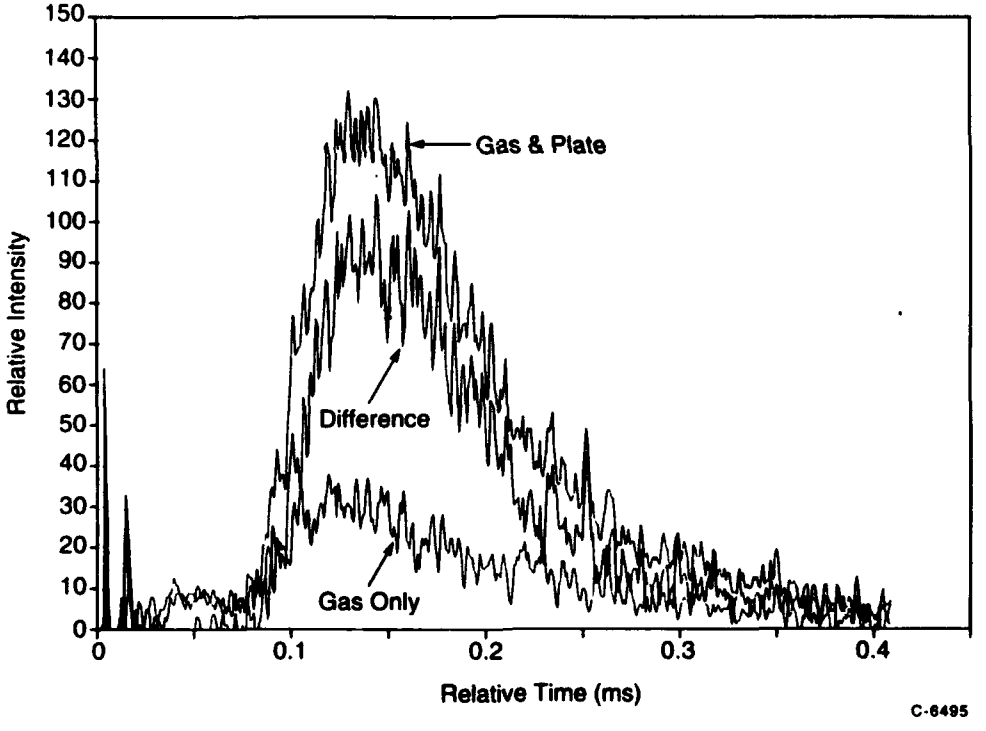

Figure 2. Observed Emission Near 630 nm, 72.5 cm Downstream of Nozzle Throat. $P_{NO} = 10^{-4}$ torr, O fluence = 3.6×10^{14} cm^2, v = 8 km/s.

The difference between these two signals, also shown on the Figure, is taken to be that due to the glow. It is of course possible that there could be some additional emission

caused by reaction between scattered O and NO, however this does not appear to be the case since no significant signal is observed after beam pulse transition.

The signal shown in Figure 2 is that observed after the intensity has reached its saturated value. To study the saturation behavior of the glow intensity we have performed such measurements as a function of NO pressure. The resulting data, integrated over pulse time, are shown in Figure 3. We note that the background pressure of these measurements was 2×10^{-6} torr so that the deduced NO pressure becomes increasingly inaccurate as we approach this limit. Note that the surface glow measurements are relatively precise until NO pressures of 10^{-4} are exceeded. At this point the gas glow begins to rise sharply and the deduced surface glow intensity begins to exhibit significant scatter. Nonetheless, the surface glow appears to be approaching saturation at this point. Shown also on Figure 3 is the evaluation of Eq. (21) under the assumption that the saturation intensity is ~ 0.50. Given the scatter in the data the comparison is reasonable. Recall that at the listed value of 2×10^{-6} torr the actual NO pressure will be much closer to zero, thus the theory provides an upper bound there.

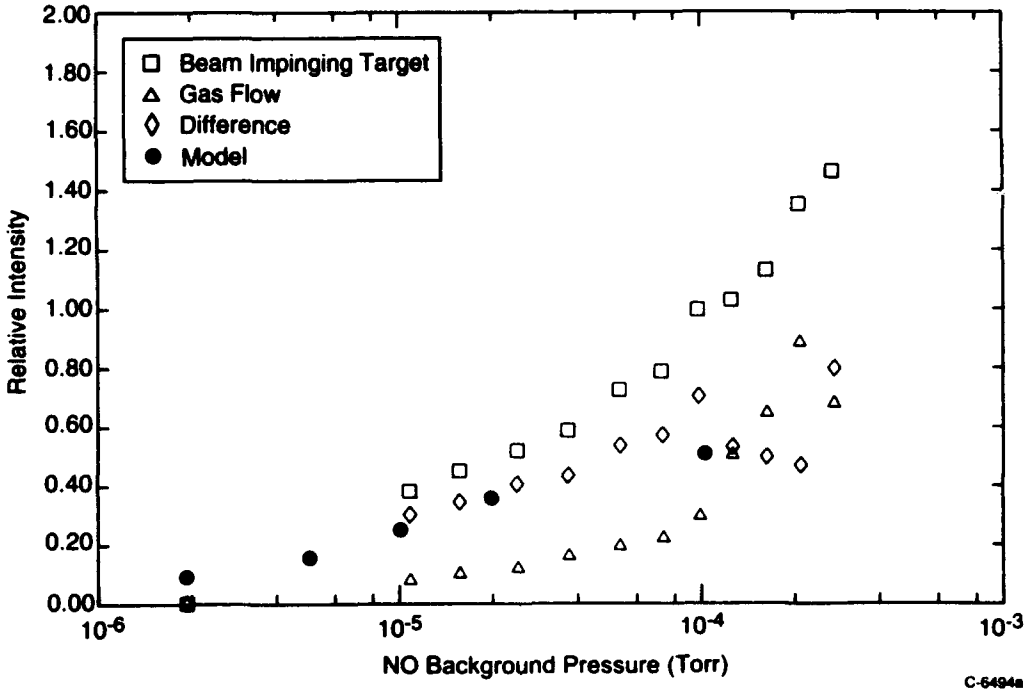

Figure 3. Observed O + NO Emission at 630 nm and 290K, 10 nm Bandpass, 2 Hz Rate, 8 km/s

The 50% saturation point occurs at $\sim 10^{-5}$ torr and thus from Eq. (22)

$$1 = 3.3 \times 10^{11} \frac{S_{NO}\, \bar{c}\, \tau_{NO}}{4\, N_s} \qquad (25)$$

where we have substituted in the NO concentration at P = 10^{-5} torr. $\therefore$ for $\bar{c}$ = 4.5 x 10^4 and $N_s \sim 3 \times 10^{15}$ cm^{-2} we have then

$$S_{NO}\tau_{NO} = 0.81s \qquad (26)$$

and, since S_{NO} cannot exceed unity, this implies that at 290 K

$$\tau_{NO} \geq 0.81s \quad .$$

This evaluation is uncertain to at least a factor of two given the scatter in the data and the arbitrariness in the specification of N_s (more properly, Eq. (2) should be used to define the quantity $S_{NO}\ \tau_{NO}/N_s$).

As a final study we examined the time history of the intensity as it approached steady state. Our object was to utilize the time dependent solution, Eq. (23), to independently evaluate S_{NO} and τ_{NO}. Our approach was to irradiate the target with the O-beam at a steady repetition frequency (initially 2 Hz) at the base pressure of 2 x 10^{-6} torr and then suddenly turn the NO flow on, rapidly reaching an equilibrium NO pressure. The observed change in intensity with time was then analyzed in terms of Eq. (23). This is not a truly "clean" experiment in that a finite time is required for the NO to equilibrate within the chamber. We estimate for our chamber dimensions and these near free molecular conditions that this equilibration time will be only a fraction of a second.

The characteristic e-fold rise times measured at several NO pressures are shown in Table 2. As can be seen, there is no discernable pressure dependence on the rise time, although there is noticeable scatter in the data. Presumably the scatter is in part relatable to the NO equilibration time but recall also that the time resolution of the measurements is 0.5s. The average observed rise time is 2.7 $\pm$ 1.0s. From Eq. (24) it could be inferred that this is the thermal desorption lifetime of NO, whence from Eq. (26), S_{NO} would be assigned the value of 0.3.

Table 2. Characteristic Glow Intensity e-fold Rise time versus NO pressure (O beam at 2 Hz)

NO BG Pressure (Torr)	$t_{1/e}$ (s)
6.2 x 10^{-6}	3.5
6.2 x 10^{-6}	2.0
1.1 x 10^{-6}	2.5
1.1 x 10^{-6}	3.0
7.0 x 10^{-5}	2.5

As a last crosscheck, we performed an additional measurement at an NO pressure of 1.1×10^{-5} torr and an O-beam repetition rate of 0.5 Hz. Fluence per pulse remained the same as in the prior measurements. In this case the characteristic e-fold time was found to be a factor of four longer than observed in the 2 Hz measurements, i.e., the e-fold time scaled inversely with the repetition rate! Clearly the rate limiting step observed in these measurements is not related to NO adsorption but rather to an oxygen atom surface interaction. This implies that the NO desorption time must be < 2.7s and therefore the sticking coefficient must be > 0.3.

Indeed, although more detailed measurements are warranted, it appears that the observed e-fold time is linearly proportional to the total O-atom fluence on the target (once the NO is introduced into the chamber). Recall the characteristic 8 km/s O-beam pulse fluence is $\sim 3.6 \times 10^{14}$. Thus at 2 Hz the observed e-fold time would correspond to a total impinging O-atom fluence of 2×10^{15} cm^{-2}, or on the order of a mono-layer.

If this observation is correct, it implies that the simple Langmuir-Hinshelwood mechanism is not consistent with our data and indeed perhaps does not provide an appropriate interpretation of the Shuttle glow. It is clear that this observed O-atom fluence dependence is not just related to O-atom build-up on the surface in sticky collisions. This is because: (1) the O-beam was running prior to NO injection presumably providing the opportunity to saturate the surface with oxygen atoms; and (2) the glow is only observed during pulses of the O-beam, so there is no glow-producing rapid reaction between surface adsorbed O and NO occurring between pulses.

We have developed a mechanistic conjecture which is consistent with our data, but presents a whole new view of the cause of shuttle glow. That is that O and NO adsorbed on the surface react to form NO_2 but that this NO_2 largely remains adsorbed to the surface perhaps through chemisorption. An additional collision with an energetic oxygen atom is then required to produce excited gaseous NO_2, either in a knockoff or exchange collision. In a way we are proposing a forced marriage between the Rideal and Langmuir-Hirshelwood mechanisms.

This hypothesis is based on limited data and must be tested out by further experiments. We do however have two additional pieces of data which are consistent with this mechanism. The first is an earlier[14] study of fast O-atom induced surface glows. In this work we pre-dosed liquid nitrogen cooled samples of Z306 separately with NO and NO_2 and then bombarded the samples with pulses of 8 km/s oxygen atoms. The resulting surface glow observations are shown in Figure 4. As can be seen the spectral shapes of the observed glows are very similar, consistent with the proposed mechanism. It would be valuable to study the time dependent glow history in an NO_2 backfill experiment. If the proposed mechanism is correct there should be no glow dependence on O-atom repetition rate inasmuch as the NO_2 will be formed on the surface prior to O-atom irradiation.

The second observation, which is unpublished, is that the steady glow intensity seems to increase significantly with increasing O-beam velocity (at the same O-beam pulse fluence)

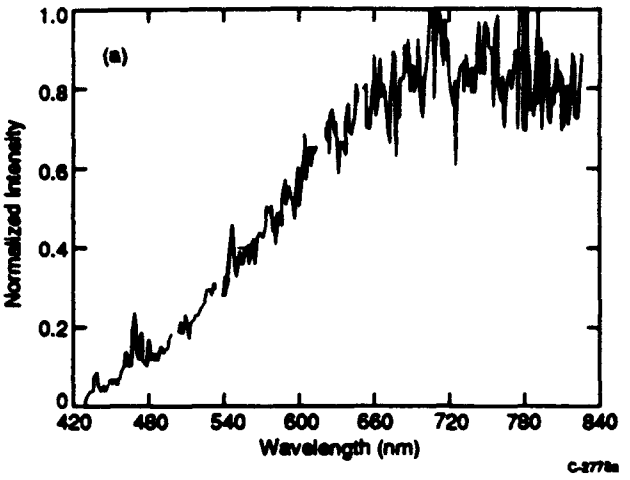

(a) NO_2-Dosed

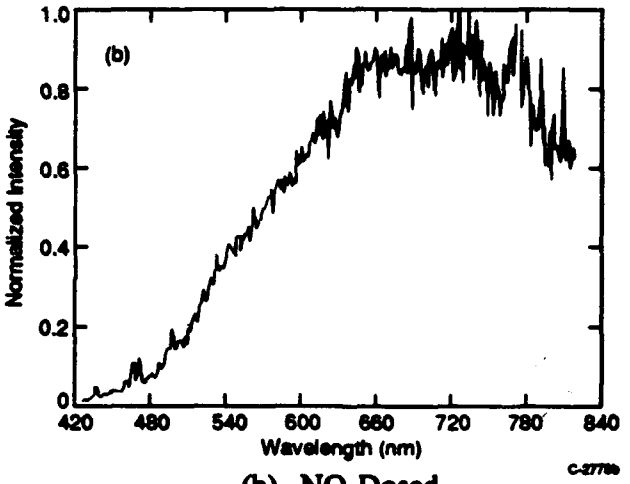

(b) NO-Dosed

Figure 4. Spectrum of glow observed upon impacting a Z306 target (liquid nitrogen cooled) with a beam of 8 km/s oxygen atoms.

This would be a surprising observation for a Langmuir-Hinshelwood mechanism, requiring that the O-atom sticking coefficient increase sizably with increasing velocity, but not unreasonable for a Rideal mechanism.

In summary, our investigation into the shock glow mechanism has produced some unanticipated experimental results. This new data, although preliminary, suggest a radically new mechanism for the glow. Alternate kinetic hypotheses may also be tenable. These mechanisms must ultimately be subjected to experimental validation tests.

2.5 References

1. Mende, S. B., R. Noble, P. M. Banks, O. K. Garriott, and J. Hoffman, Measurement of vehicle glow on space shuttle, *J. Spacecr.*, *21*, 374 1984.

2. Mende, S. B., G. R. Swenson and E. J. Llewellyn, Ram glow: interaction of space vehicles with the natural atmosphere, *Adv. Space Res.*, *8*(1), 229, 1988.

3. Garrett, H. B., A. Chutjian, and S. Gabriel, Space vehicle glow and its impact on spacecraft systems, *J. Spacecr. 25*, 321, 1988.

4. Ahmadjian, M., D. E. Jennings, M. J. Mumma, F. Espenak, C. J. Rice, R. W. Russell and B. D. Green, Infrared spectral measurements of space shuttle glow, *Geophys. Res. Lett.*, *19*, 989, 1992.

5. Conway, R.R., Meier, R.R., Strobel, D.F., and Huffman, R.E., "The Far Ultraviolet Vehicle Glow of the S3-4 Satellite," *Geophys. Res. Lett.* **14**, 628 (1987).

6. Swenson, G.R. and Meyerott, R.E., "Spacecraft Ram Cloud Exchange and N_2 LBH Glow," *Geophys. Res. Let.* **15**, 245 (1988).

7. Meyerott, R.E. and Swenson, G.R., "A Surface Chemistry Model for the Production of N_2 LBH Spacecraft Glow," *Planet. Space Sci.* **38**(4), pp. 555-566, 1990.

8. Meyerott, R.E. and Swenson, G.R., "N_2 Spacecraft Glows from $N(^4S)$ Recombination," *Planet. Space Sci.*, **39**(3), pp. 469-478, 1991.

9. Caledonia, G.E., Holtzclaw, K.W., Krech, R.H., Sonnenfroh, D.M., Leone, A., and Blumberg, W.A.M., "Mechanistic Investigations of Shuttle Glow," J. Geophys. Res. 98, 3725 (1993).

10. Yee, J.H. and Abreu, V.J., "Visible Glow Induced by Spacecraft-Environment Interaction," *Geophys. Res. Lett.* **10**, 126 (1983).

11. Swenson, G.R., Mende, S.B., and Llewellyn, E.J., "The Effect of Temperature on Shuttle Glow," *Nature* **323**, 519 (1986).

12. Caledonia, G.E., Krech, R.H., and Green, B.D., "A High Flux Source of Energetic Oxygen Atoms for Material Degradation Studies," AIAA J. 25/1, 59 (1987).

13. Caledonia, G.E., Holtzclaw, K.W., Green, B.D., Krech, R.H., Leone, A., and Swenson, G.R., "Laboratory Investigation of Shuttle Glow Mechanisms," Geophys. Res. Lett. 17(11), p. 1881-1884, October 1990.

14. Swenson, G.R., Leone, A., Holtzclaw, K.W., and Caledonia, G.E., "Spatial and Spectral Characterization of Laboratory Shuttle Glow Simulations," J. Geophys. Res. 96, 7603 (1991).

15. Sonnenfroh, D.M. and Caledonia, G.E., "Collisional Desorption of NO by Fast O-Atoms," J. Geophys. Res. 98, 21,603 (1993).

3. SURFACE GLOWS ON HYPERSONIC VEHICLES

The intensities of surface glows observed in rarefied hypersonic flows will, in general, reflect effects due to a variety of phenomena and, thus, it is difficult and dangerous to extrapolate the limited database to new conditions.

Specifically, the species which produce the glow, e.g., NO_2, N_2^*, will generally be formed from precursors created through interactions between ambient species incident and scattered from the spacecraft surface, thus, both ambient density and vehicle size will contribute to the flow intensity. Furthermore, the radiating species are formed through surface catalyzed reactions and, thus, parameters affecting the surface's ability to retain the precursors become important. These parameters include surface accommodation coefficient, temperature, and saturation level.

It is clear that such scaling cannot be performed without a proposed mechanism for the chemical reaction sequence responsible for the glow. Even with a postulated mechanism, the scaling relationship will involve several unevaluated parameters. Several mechanisms have been proposed, however, for visible and UV glows, e.g., Refs. 15-18 among many others, and we will later provide estimates of anticipated glow intensities for the Skipper mission, uncertainties notwithstanding.

In this interim report we provide a brief summary of visible UV/glow measurements along with the relevant vehicle parameters.

We will first examine the visible "shuttle" glow which has the largest database. This is a continuum emission covering the spectral region from 400 nm to the infrared. The emission has been shown to result from surface catalyzed recombination of O and NO, with the oxygen atoms being an ambient species and the NO presumably being formed around the vehicle, see Ref. 17. A comparison between flight measurement and laboratory data is shown in Figure 5, excerpted from Ref. 17. We will present data at 730 nm and this can be scaled to other wavelengths using this measured spectral shape.

Although there are numerous measurements of the shuttle glow, many of these are uncalibrated. Furthermore, the measurements are generally made along the surface so as to maximize signal and under conditions where the surface need not be fully exposed to the ram flow. The appropriate viewing geometry for our interest is perpendicular to the surface and into the ram flow. The measurements can be corrected for these effects using scaling laws (i.e., ram angle scaling, glow depth, etc.) developed from the larger database. Swenson et al.[17] have performed these adjustments and the resulting intensities perpendicular to the surface as deduced from data taken on shuttle flights STS-8, STS-9, and STS-41G are shown in Figure 6. Swenson et al.[17] point out that this data can further be correlated by accounting for differences in the surface temperatures on these flights.

The intensities are reported in Rayleighs/Å (R/Å). The Rayleigh is a unit of column intensity corresponding to 10^6 photons/cm^2. Data from other flights can be used to infer

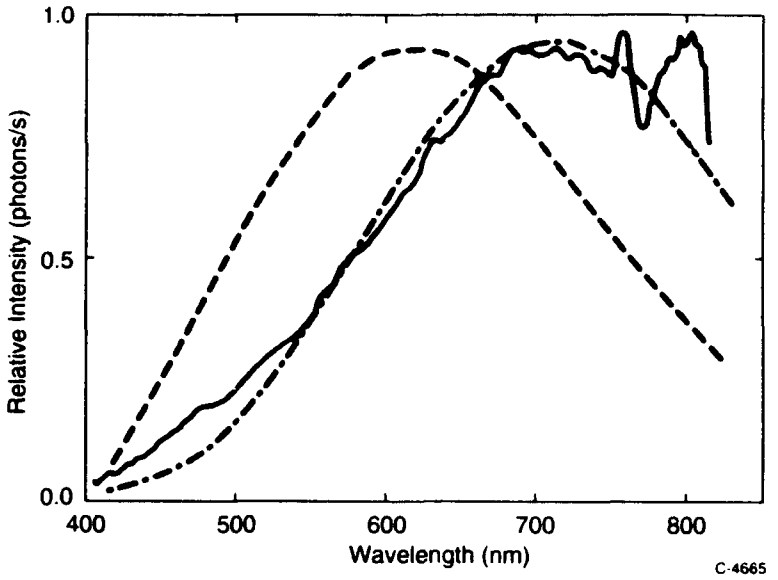

Figure 5. Comparison of laboratory and space shuttle glows. (solid line) Shuttle glow observed[19] on STS-38; (dashed-dotted line) laboratory measurements of glow from 8 km/s oxygen atoms interacting with NO-dosed surfaces;[20] (dashed line) laboratory measurements of glow from 8 km/s oxygen atom interacting with a thermal gaseous jet of NO.[20]

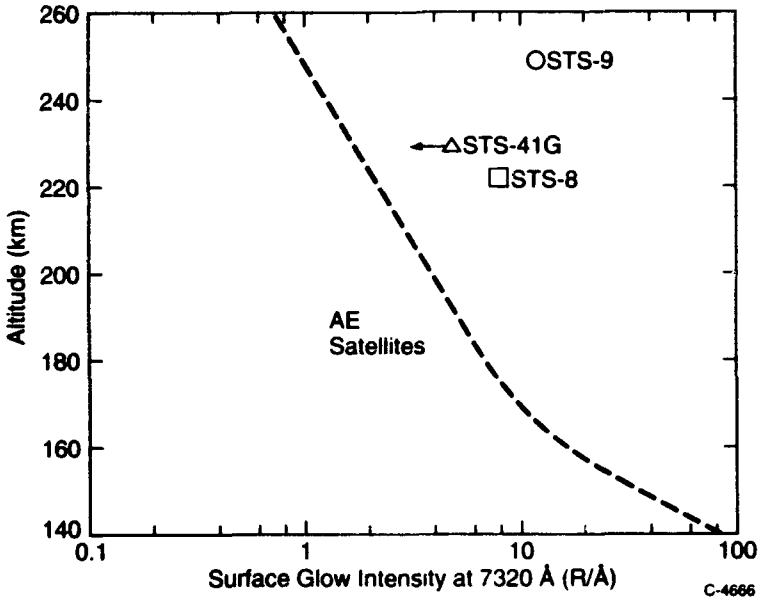

Figure 6. Summary of visible glow intensity observations versus altitude. All results corrected to a line of sight perpendicular to the surface and in the ram direction.

relative scaling with altitude. In general, it is believed that the glow scales approximately linearly with the O-atom density at shuttle altitudes. (An upper bound estimate of the 7320Å glow intensity of <2 R/Å is available for an altitude of 320 km from STS-41G data. This is probably a strong upper bound.)

The only other significant database is from the atmospheric explorer satellites and the generic altitude dependence on that data is also shown in Figure 6, as taken from Ref. 21. Swenson et al.[17] point out that the surface temperature of the AE-C satellite is higher than that for the shuttle and that this can account for the lower intensities. Recall, however, that platform size and materials are also different. Note the break in the slope of intensity with altitude at about 160 km presumably has kinetic implications.

There were also limited observations of an ultraviolet glow on AE.[21] Reported intensities at 3371Å were 0.6 R/Å at approximately 170 to 175 km and 5 R/Å at approximately 140 to 145 km. A shuttle study at 320 km[22] reported that any UV emission (<3200Å) fell below the zodiacal background.

A significant surface glow in the VUV has been reported by Conway et al.[23] as observed on the S3-4 satellite. This emission, observed between 1300 to 1700Å, arises from the N_2 LBH bands. The observed spectral distribution, as compared to a synthetic spectrum, is shown in Figure 7. This glow exhibits a very strong altitude dependence as shown in Figure 8. This data is integrated over the whole bandpass, given the observed structured in the spectra (Figure 7). Again the shuttle data[22] shows no intensity above zodiacal background at these wavelengths for an altitude of 320 km. This latter observation is not inconsistent with an extrapolation of the data of Figure 7. Most recently, Morrison et al.[10] have reported an upper band on LBH emissions at 250 km to be <5.3R, again consistent with an extrapolation of the data in Figure 7. This evaluation was from data taken on STS-61C. Upper bounds for radiation for other band systems falling between 1600 to 3200Å are also included in this work

Although an exhaustive literature search has not been performed, the data presented above provides a reasonable summary of observed surface glow intensities in rarefied orbital flow.

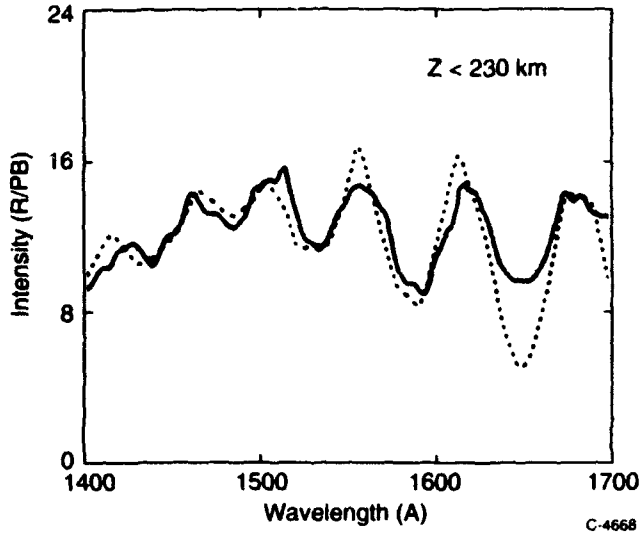

Figure 7. Nighttime observation from S3-4 satellite on orbit 373. Average spectrum for data below 230 km in Rayleighs/passband. Dashed curve is best fit synthetic LBH spectrum. All observations are nadir-viewing with a resolution of 30Å measured at Lyman alpha. Excerpted from Ref. 23.

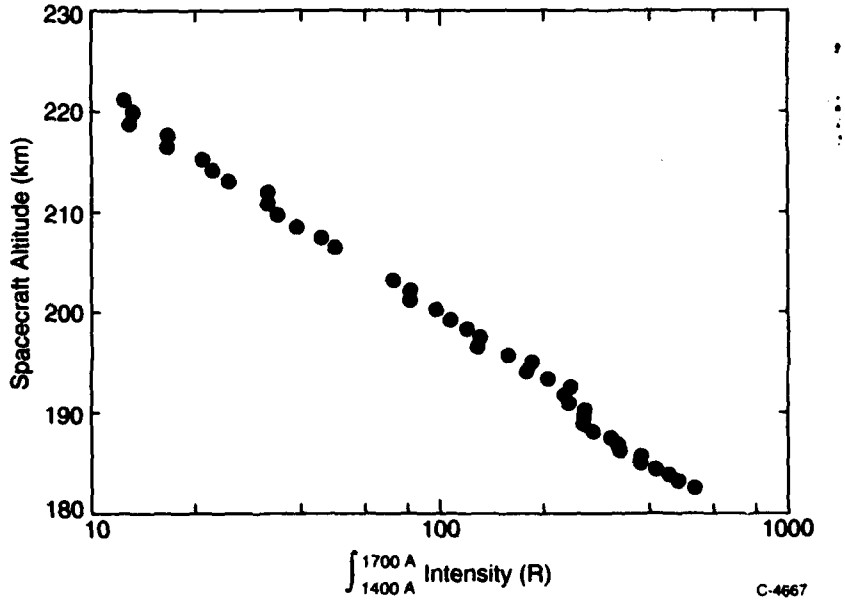

Figure 8. Total intensity in Rayleighs between 1400 and 1700Å versus S3-4 satellite altitude. Excerpted from Ref. 23.

3.1 References

1. Swenson, G.R., Mende, S.B., and Llewellyn, E.J., "The Effect of Temperature on Shuttle Glow," *Nature* **323**, 519 (1986).

2. Swenson, G.R. and Meyerott, R.E., "Spacecraft Ram Cloud Exchange and N_2 LBH Glow," *Geophys. Res. Let.* **15**, 245 (1988).

3. Caledonia, G.E., Holtzclaw, K.W., Krech, R.H., Sonnenfroh, D.M., Leone, A., and Blumberg, W.A.M., "Mechanistic Investigations of Shuttle Glow," *J. Geophys. Res.* **98**, 3725 (1993).

4. Greer, W.A.D., Pratt, N.H., and Stark, J.P.W., "Spacecraft Glows and laboratory Luminescence: Evidence for a Common Reaction Mechanism," *Geophys. Res. Lett.* **20**, 731 (1993).

5. Viereck, R.E., Murad, E., Pike, C., Mendes, S., Swenson, G., Culbertson, S.L., and Springer, R.C., "Spectral Characteristics of the Shuttle Glow," *Geophys. Res. Lett.* **19**, 1219 (1992).

6. Caledonia, G.E., Holtzclaw, K.W., Green, B.D., Krech, R.H., Leone, A., and Swenson, G.R., "Laboratory Investigation of Shuttle Glow Mechanisms," *Geophys. Res. Lett.* **17**, 1881 (1990).

7. Yee, J.H. and Abreu, V.J., "Visible Glow Induced by Spacecraft-Environment Interaction," *Geophys. Res. Lett.* **10**, 126 (1983).

8. Tennyson, P.D., Feldman, P.D., and Henry, R.C., "Search for Ultraviolet Shuttle Glow," *Adv. Space Res.* **7**, 207 (1987).

9. Conway, R.R., Meier, R.R., Strobel, D.F., and Huffman, R.E., "The Far Ultraviolet Vehicle Glow of the S3-4 Satellite," *Geophys. Res. Lett.* **14**, 628 (1987).

10. Morrison, D., Feldman, P.D., and Henry, R.C., "Upper Limits on Spacecraft-Induced Ultraviolet Emissions from the Space Shuttle (STS-61C)," *J. Geophys. Res.* **97**, 1633 (1992).

4. SENSOR ISSUES RELATED TO THE HIGH VELOCITY MISSILE

The HVM system is being designed with the capability of intercepting a missile in its boost phase at a standoff distance of approximately 400 km. This requires intercept at 40 to 60 km, with missile speeds of 6 to 10 km. A brief assessment of sensor survival/viability is provided below, assuming an infrared seeker band.

There are at least three key interrelated issues in this system concept: (1) will the nosetip survive over the intercept distance; (2) will the window or its protective appendages survive and can the target be observed against the emission from the heated window material; and (3) what additional complications arise from emissive and refractive effects occurring in the inviscid shock and (possibly turbulent) boundary layer.

We have made some quick numbers to estimate nosetip survival using a simple Q* model. For simplicity we did calculations of the range for nosetip erosion (2 cm) at constant altitude as a function of velocity. These are shown in Figure 9 where the 40 to 60 km altitude range is highlighted. Note for example that the nosetip survival range is limited for operation above 6 km/s at altitudes below 30 km. These calculations can, of course, be done more carefully for a range of engagement trajectories so as to properly delineate where this effect dominates.

It is assumed that the seeker window is forward looking but off of the nose. There are lots of tricks to ensure window survival (and cooling) that have been examined for lower velocity interceptors. These include flow separators, transpiration cooling, etc. Again any structures to channel flow must also survive the high heat transfer environment. There are also tricks to "see" through the background of a warm window, for example by dithering the optic on and off the target. There are a few back of the envelope things that can be done here but this issue requires both system design and more detailed flow analysis.

Lastly is the emission/refraction from the inviscid shock layer/boundary layer. If there is nose ablation there will be CO and CO_2 emissions in the boundary layer in the 4 to 5 μm region. At elevated velocities the dominant shock layer IR emitter will be neutral and ionic Bremsstrahlung which is a continuum emission. As an example we've made one estimate of emission near the nose region at 40 km and 10 km/s velocity. The nose flow will be near equilibrium for these conditions. Assuming equilibrium and a shock thickness of 0.1 Rn we find that the ionic and neutral contributions are about equal and the total emission in the 3 to 4 μm region would be $\approx$0.1 W/cm^2-sr, roughly equivalent to an 800 K blackbody. Note that Bremsstrahlung emission scales as density squared so that this intensity will increase significantly with decreasing altitude. Alternatively, since it depends on the ionization level, this emission intensity will decrease with decreasing velocity. Lastly, with increasing intercept altitude, non-equilibrium chemistry will become more important but intensities will be lower.

One last point with respect to ionic emissions. There will also be a 4 μm band-like structure which is due to a Rydberg transition, which is generally as intense as the neutral

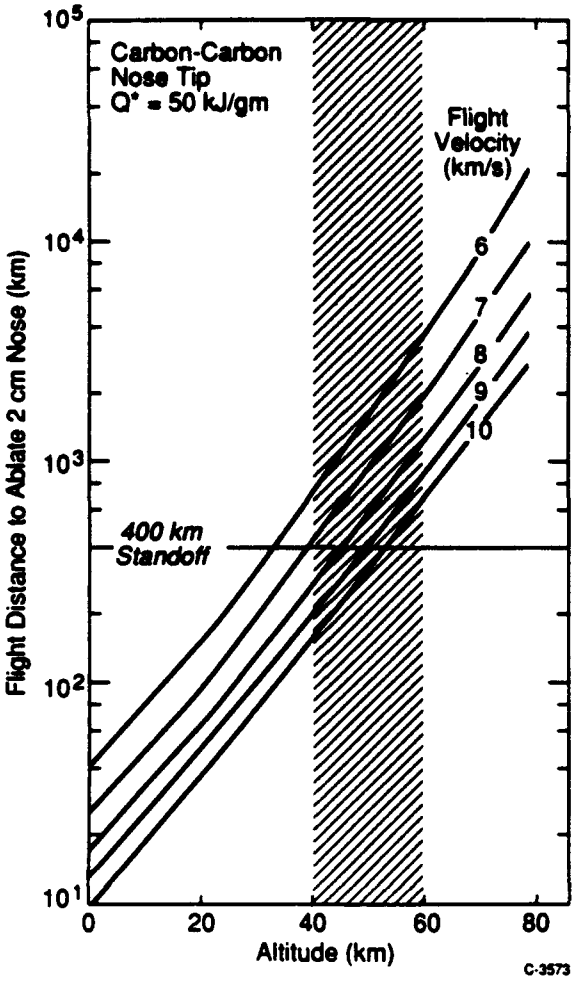

Figure 9. Predicted nose ablation (r = 2 cm) for hypersonic flight at constant altitude.

Bremsstrahlung emission. A brief review of Bremsstrahlung radiation phenomenology is provided below.

Bremsstrahlung Radiation

Bremsstrahlung (breaking radiation) is a continuum radiation (absorption) process which results from electron interactions with ions and molecules. Basically, the Coulomb interaction provides an acceleration to the electron and allows radiation to occur. The interaction takes two forms, free-free (ionic) and neutral, i.e.,

$$x^+ + e \rightarrow x^+ + e + h\nu \qquad (27)$$

$$x + e \rightarrow x + e + h\nu \qquad (28)$$

The neutral interaction (28) occurs through acceleration resulting from force due to the induced dipole/quadropole in the neutral molecule.

In the classical theory, the scaling laws are the same for processes (27) and (28) and, as a general rule of thumb, ionic Bremsstrahlung will dominate at ionic concentrations $\gtrsim$ 1% while neutral Bremsstrahlung dominates at lower ionic concentrations. Figure 10 provides a plot of equilibrium electron mole fraction behind an incident shock at 40 km altitude. The ionic concentration exceeds 1% at V = 9.25 km/s. Note that equilibrium ionic concentrations will be higher at the stagnation point.

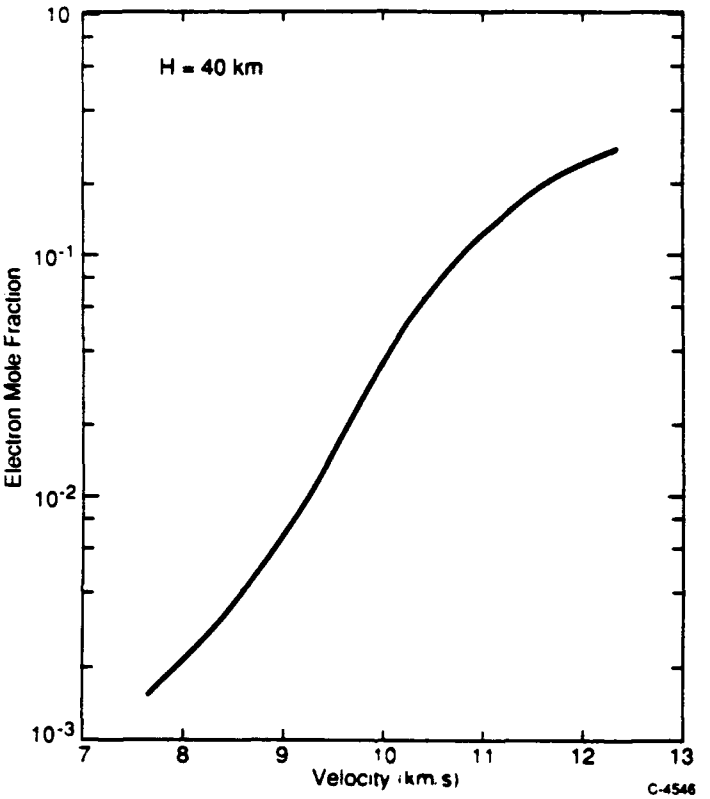

Figure 10. Equilibrium electron mole fraction behind an incident shock versus velocity.

The intensity per unit wave number due to free-free continuum emission is given by the simple relationship

$$I_{\lambda,ff} \propto N_e N_i z_{ff}^2 \lambda^{-2} e^{-hcv/kT} \tag{29}$$

where N is density and subscripts e and i refer to electron and ion. z_{ff}^2 is an effective charge which is near unity. There is an additional contribution to the continuum due to free-bound transitions. Including this effect is the equivalent of dropping the exponential term from Eq. (29). There are also discrete bound-bound transitions which can appear in the spectrum.

For neutral Bremsstrahlung, the equivalent relationship to Eq. (29) is

$$I_{\lambda,n} \propto N_e N z_{eFf}^2 \lambda^{-2} e^{-hcv/kT} \tag{30}$$

where N is now total density and z_{eFf}^2 is an effective charge which will vary from gas to gas but is $O(10^{-2})$. The work of Taylor and Caledonia[24] remains the standard evaluation of neutral Bremsstrahlung in the IR. An example result from this work measured behind a reflected shock in nitrogen is shown in Figure 11. (The dashed portions of the data may be neglected.) This measured intensity shows the classic λ^{-2} dependence. Open areas correspond to emission from bound-bound transitions, i.e., Rydberg states, with the 4 μm feature being prominent in many gases.

This type of equilibrium measurement can be made readily in a 2 in. diam combustion driven shock tube. Impurities are not an issue given the strong continuum intensity in the IR.

Note that Bremsstrahlung emission scales as the square of density as well as strongly with temperature. For velocities $\lesssim$9 km/s and pressures above 1 Torr, these emissions can exceed air band emission in the visible. They will dominate in the infrared at even lower velocities.

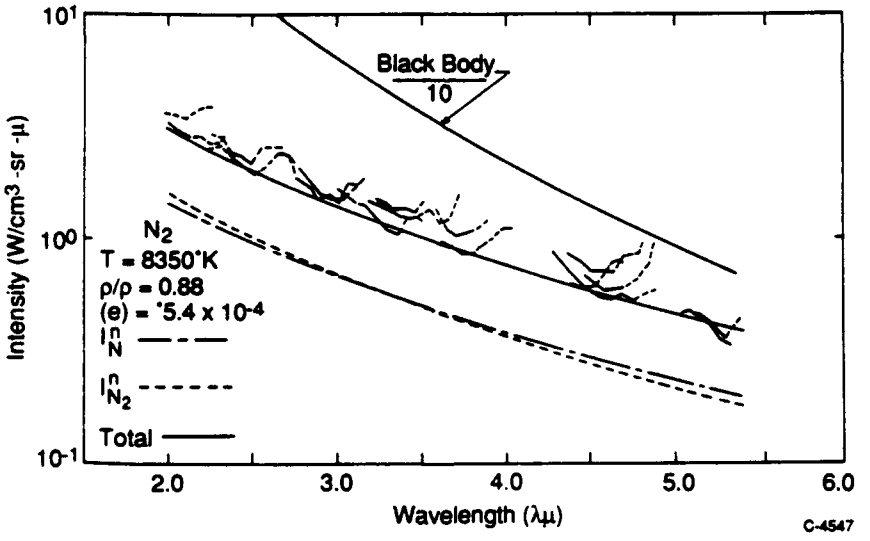

Figure 11. Composite absolute spectral intensity for pure N_2 shock heated to 8350 K. The dashed areas of data indicate regions suspected of line radiation. The lines represent calculations of the neutral Bremsstrahlung intensity for N (dot-dash), N_2 (dash), and total including Kramers (solid).

5. ACKNOWLEDGEMENTS

The heat transfer calculations presented in Section 3 were performed by Dr. Hartmut Legner.

APPENDIX A

(PSI-VG93-103)
(Reprinted in its entirety)

RAREFIED FLOW SURFACE GLOWS: IR, VISIBLE, UV, VUV

George E. Caledonia
Physical Sciences Inc.

29 April 1993

Presented at Missile Signatures Meeting
NASA Ames Research Center

RAREFIED FLOW SURFACE GLOWS: IR, VISIBLE, UV, VUV

George Caledonia
Physical Sciences Inc.

29 April 1993

Presented at Missile Signatures Meeting
NASA Ames Research Center

RADIATION PRODUCING MECHANISMS
Rarefied Flow/Hypersonic Vehicle Interactions

T-16435

- Surface catalyzed reactions
  - $O + NO(S) \rightarrow NO_2^*$
- Ambient species interaction with outgassed or scattered species
  - $O + N_2 \rightarrow NO^* + N$
  - $O^+ + H_2O \rightarrow H_2O^+ + O;\ H_2O^+ + e \rightarrow OH(A) + H$
- Ambient species chemical reactions with surfaces
  - $O + C(S) \rightarrow CO^*$
- Secondary reactions with the subsequent soup

THE SHUTTLE GLOW

T-8604

- Orange glow observed over ram surfaces in LEO
  — $\cos\theta$ law
- Scales with density
- Scales inversely with surface temperature
- Proposed mechanism – surface mediated NO_2 recombination

★ See Garrett et al., J. Spacecraft 25, 321 (1988)
Swenson et al., Nature 323, 519 (1986)

LABORATORY STUDY

T-8605

- Test postulate for surface mediated NO_2 glow
- Use PSI fast O-atom source
- Irradiate NO-doped targets (mono-layer doping)
  - — Ni, Al, Z306
  - — 77 K, 300 K
- Observe intensity, spectral shape of luminescence
- Diagnostics
  - — Scanning monochromator
  - — Imaging spectrometer

EXPERIMENTAL APPARATUS

T-8607

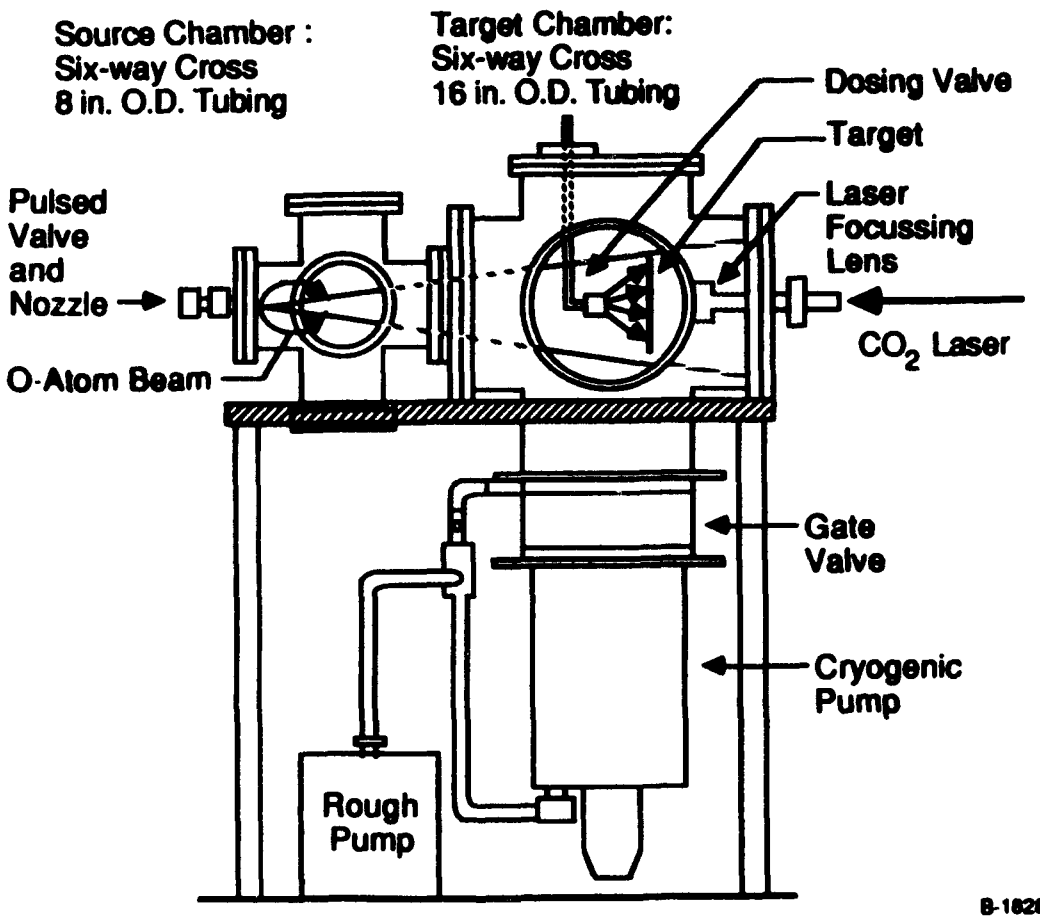

RANGE OF O-BEAM OPERATING CHARACTERISTICS

T-14097

Beam Area	-	10 to 10^3 cm^2, ~flat radial profile
Beam Flux/Pulse	-	up to 10^{15} cm^{-2} at an area 10^3 cm^2
Pulse Duration	-	30 to 100 μs
Velocity	-	5 to 12 km/s (selectable), ±15% spread
Atomic Content	-	>80% at 8 km/s
Ion Content	-	<1% at 8 km/s controllable

VISIBLE GLOW RESULTS
COMPARISON OF LABORATORY AND SPACE SHUTTLE

T-14671

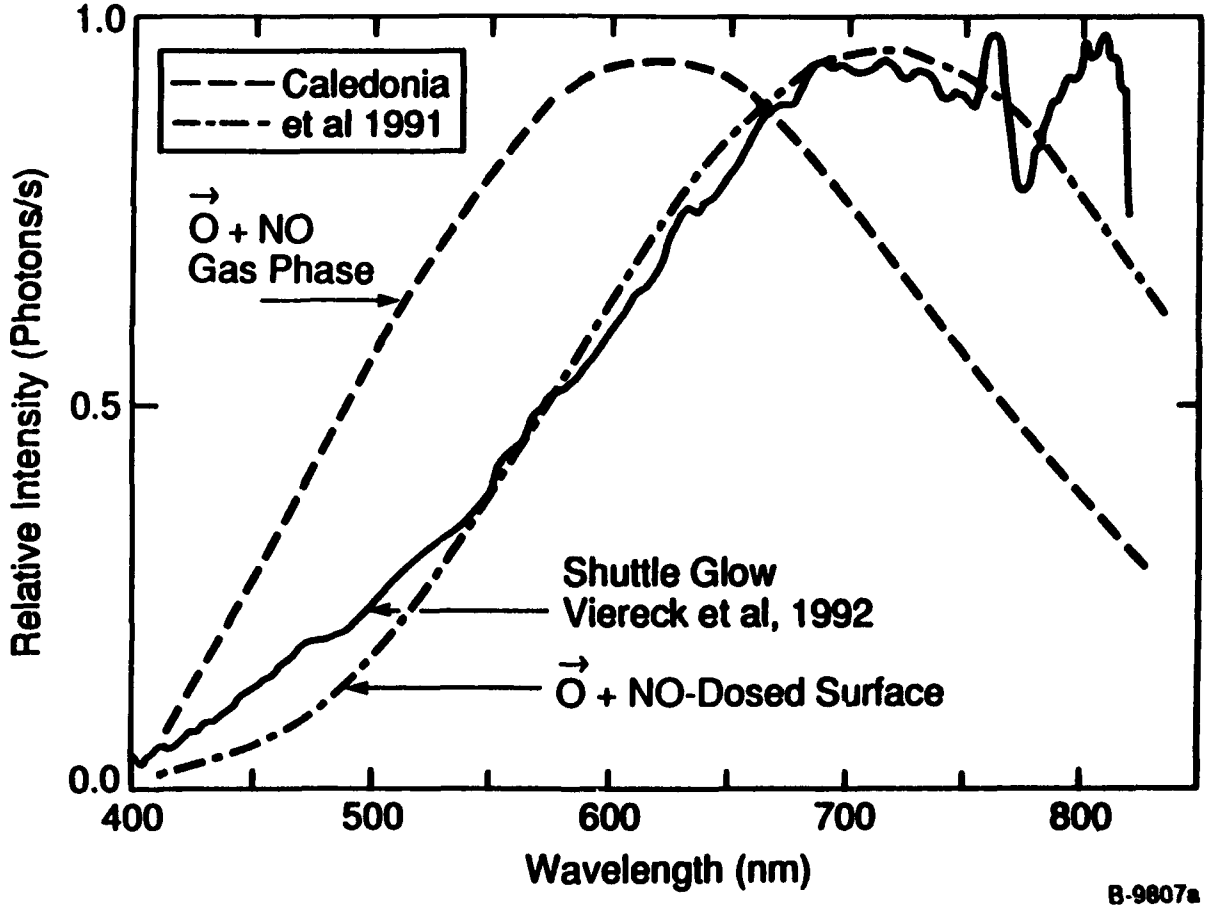

THE VISIBLE GLOW EXTENDS TO THE IR

T-16436

- PSI laboratory studies on various materials (Fraser and Gelb)

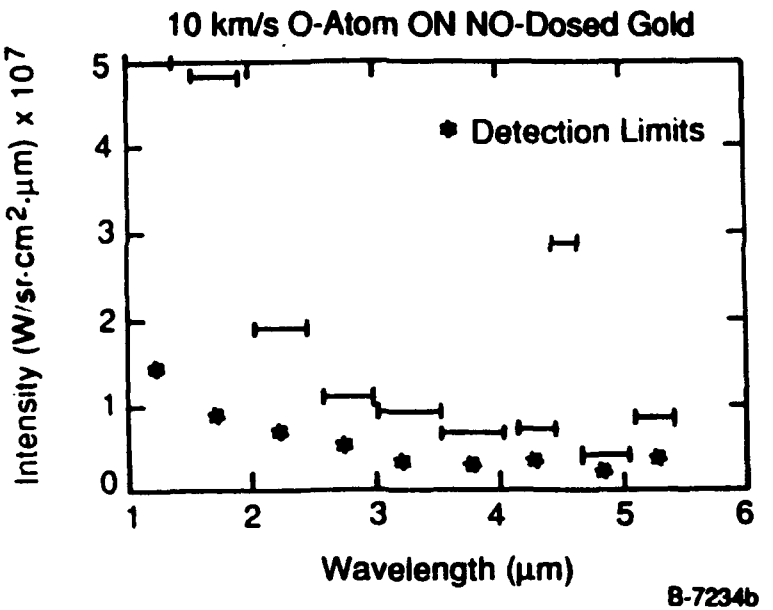

- Verified in recent Shuttle SKIRT/GLOS experiments (Ahmadjian and Green)

WHERE DOES THE NO COME FROM?

T-14640

$$O \rightarrow \leftarrow N_2$$

- Reaction between ambient species - incoming

$$O + \text{scattered } N_2$$

- Potential velocity range of interaction is 8 to 16 km/s

- Study using O-atom source in crossed beam experiment
  - — Single collision
  - — IR radiation

EXPERIMENTAL CONFIGURATION

T-3863

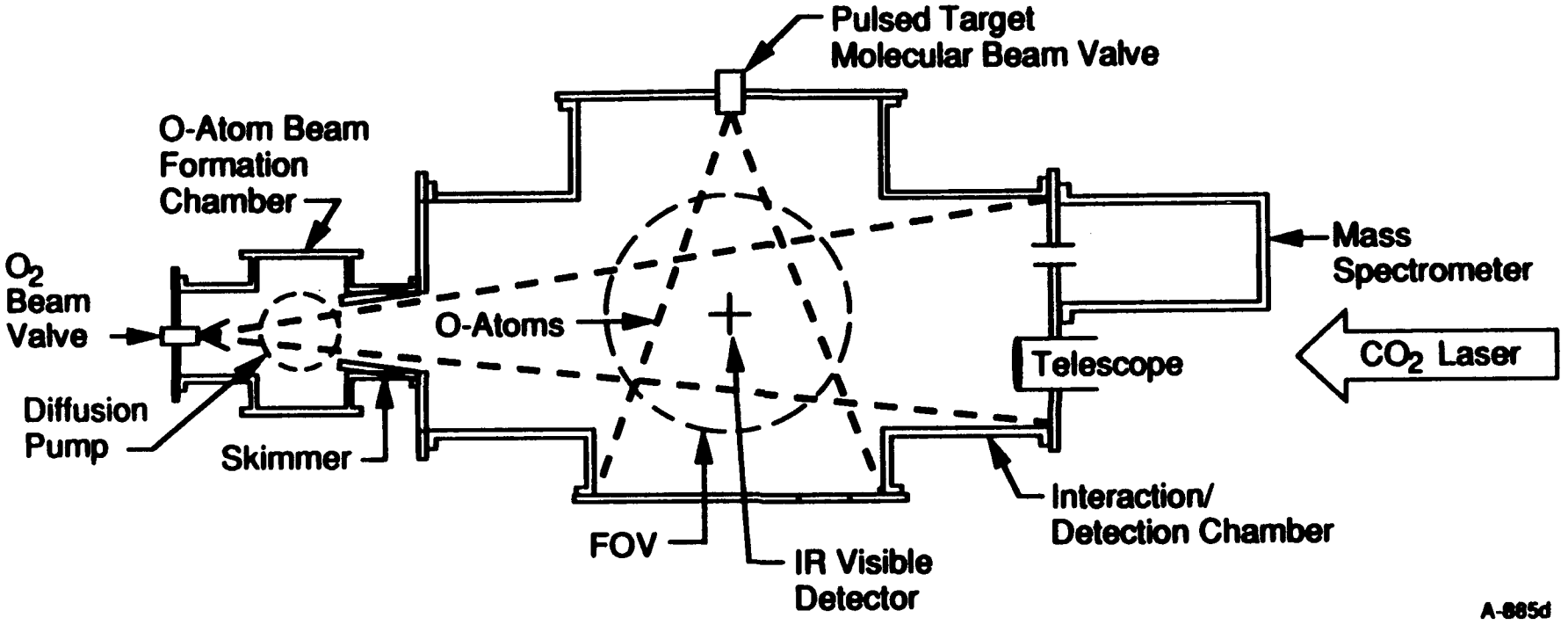

A-885d

- Interaction Region
  - — O, target gas densities ~4 x 10^{13} cm^3
  - — ~75 μs interaction time

EFFECTIVE EXCITATION CROSS SECTIONS VERSUS O-ATOM VELOCITY

$O + N_2 \rightarrow NO(V,J) + N$

T-14641

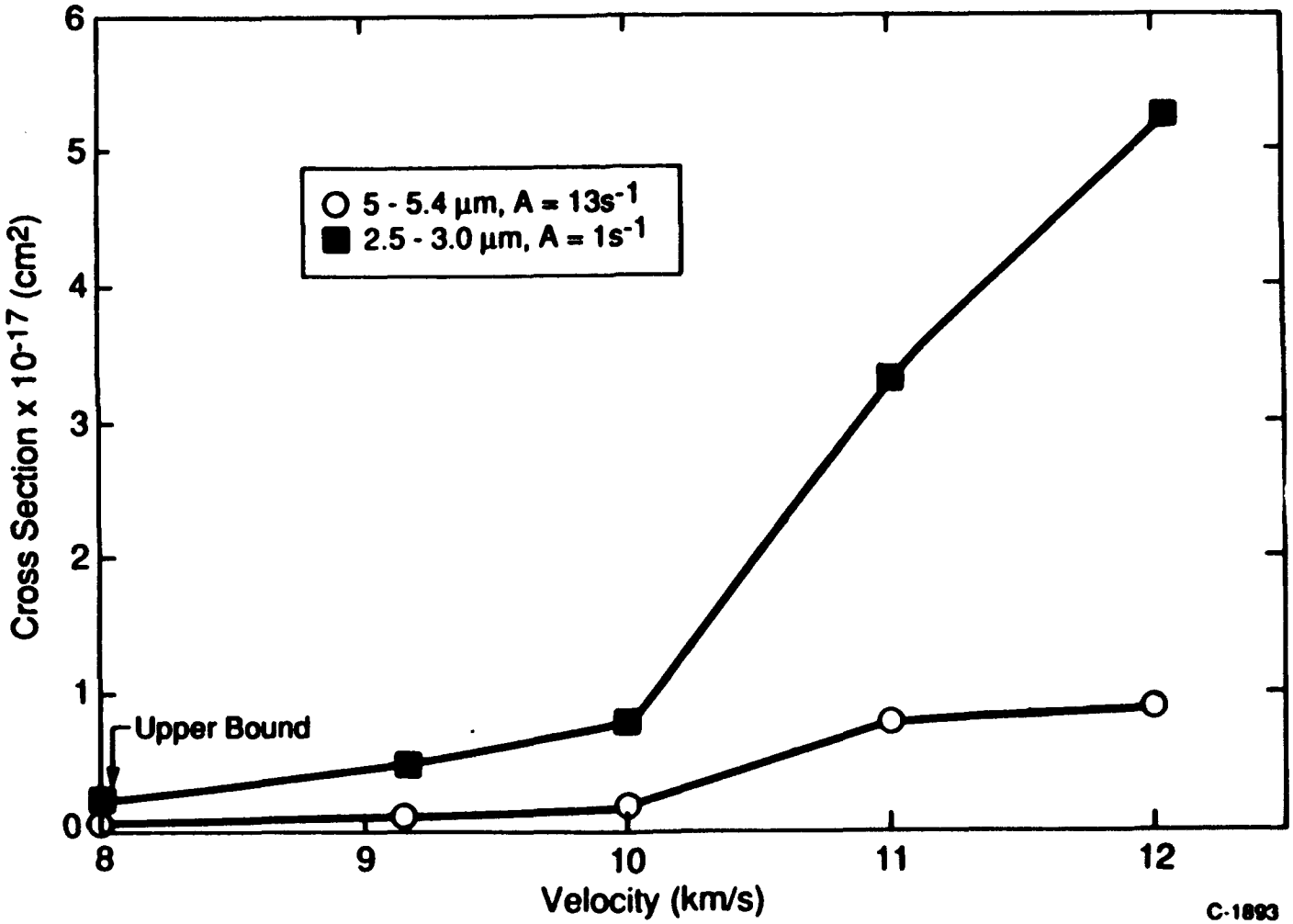

CONTINUUM UV GLOW

T-16437

- UV continuum not observed to date in Shuttle flight experiments (see Yee and Abreu, however)
  - — One laboratory experiment observed both UV and visible glow due to NO

- PSI has investigated UV glow, bombarding NO-dosed surfaces with fast O and N/N_2 beams

OBSERVED LABORATORY UV GLOW FROM ORIENT et al., Phys Rev. A 45, 2998 (1992)

T-14643

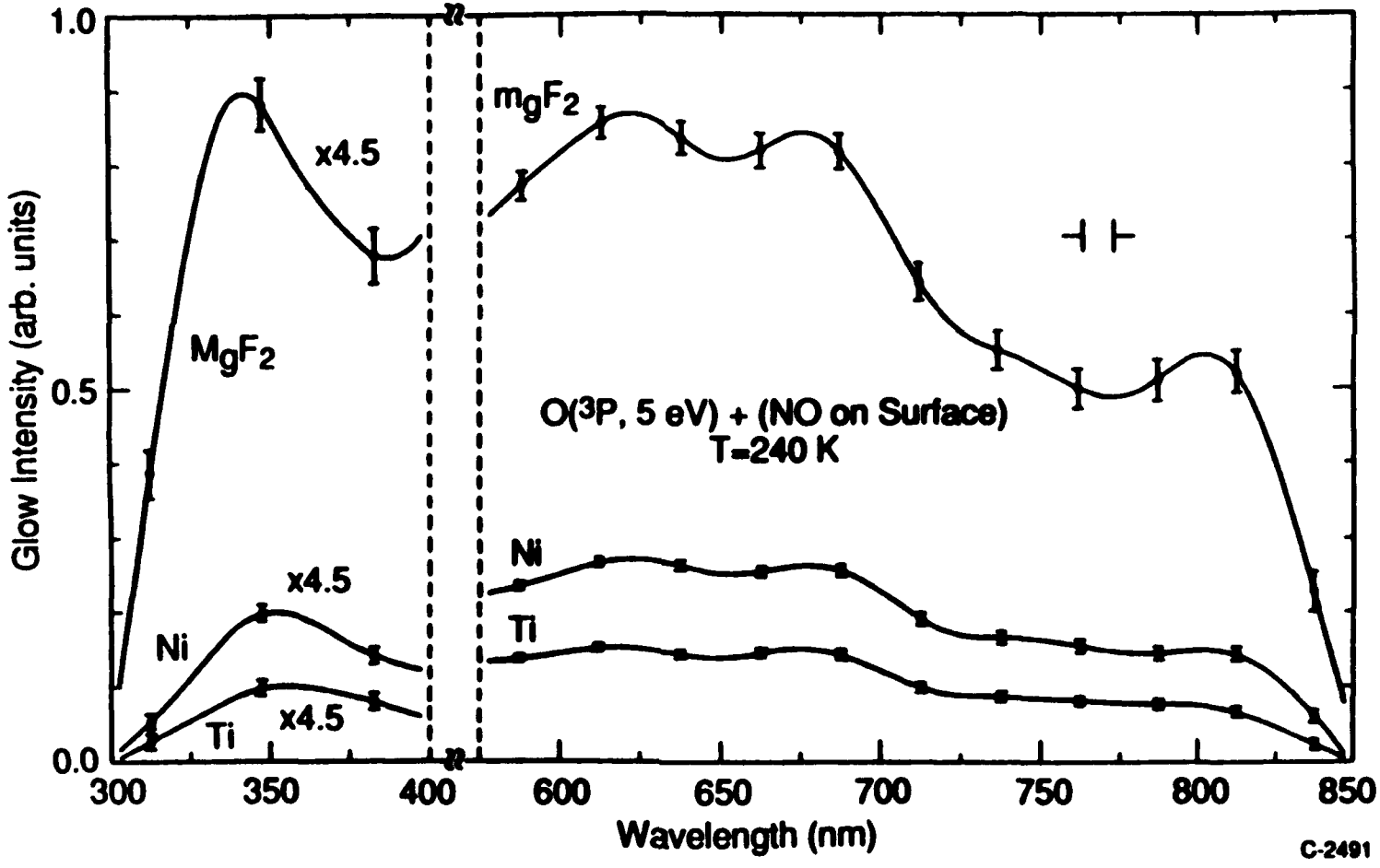

PSI STUDY
OBSERVED GLOW ABOVE COPPER SURFACE
O-BEAM, 8 km/s

T-16438

(Integrated Over 128 Pulses)

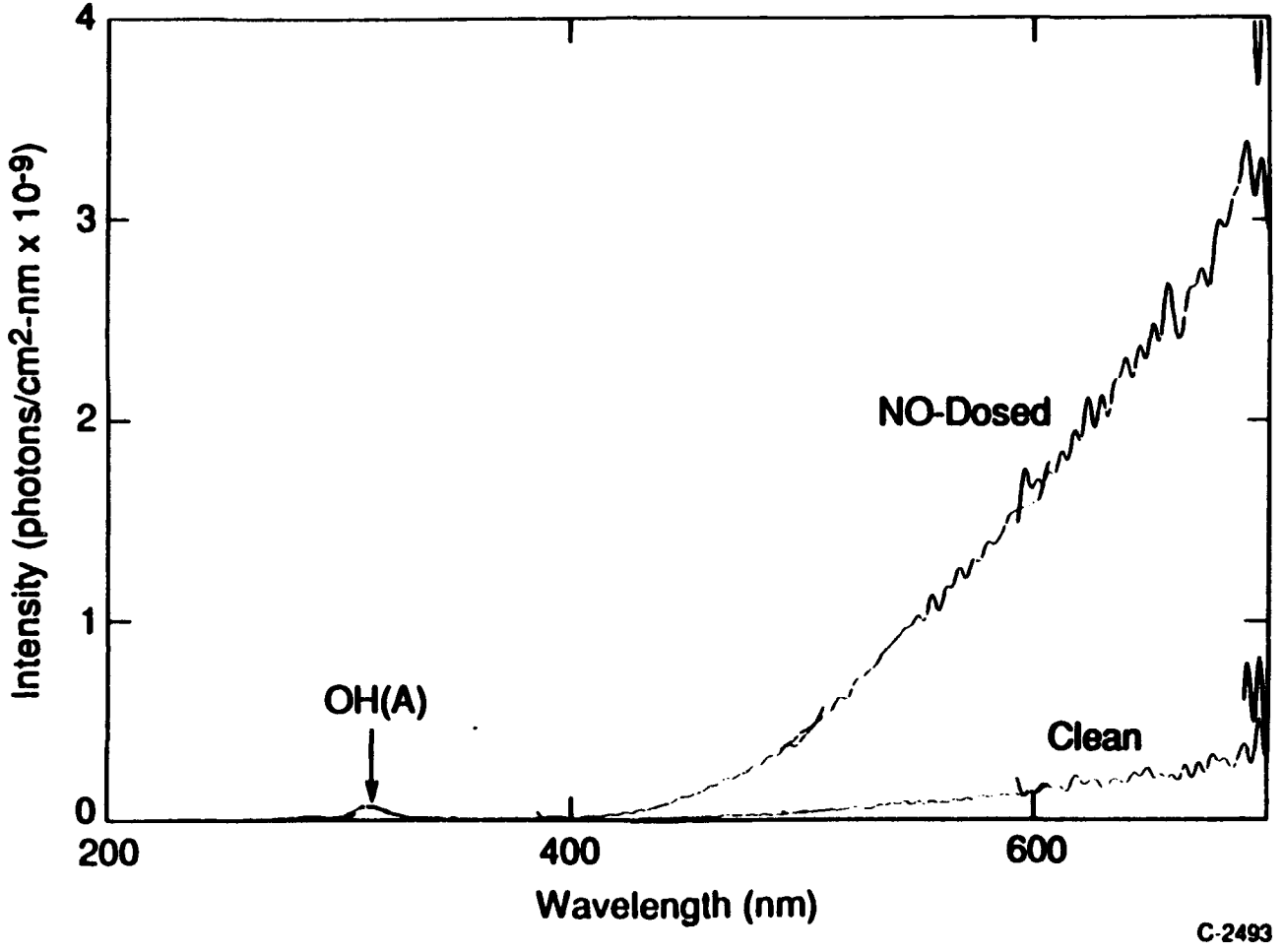

C-2493

PSI STUDY
OBSERVED GLOW ABOVE COPPER SURFACE
N/N_2 BEAM, 8 km/s

T-16439

(Integrated Over 128 Pulses)

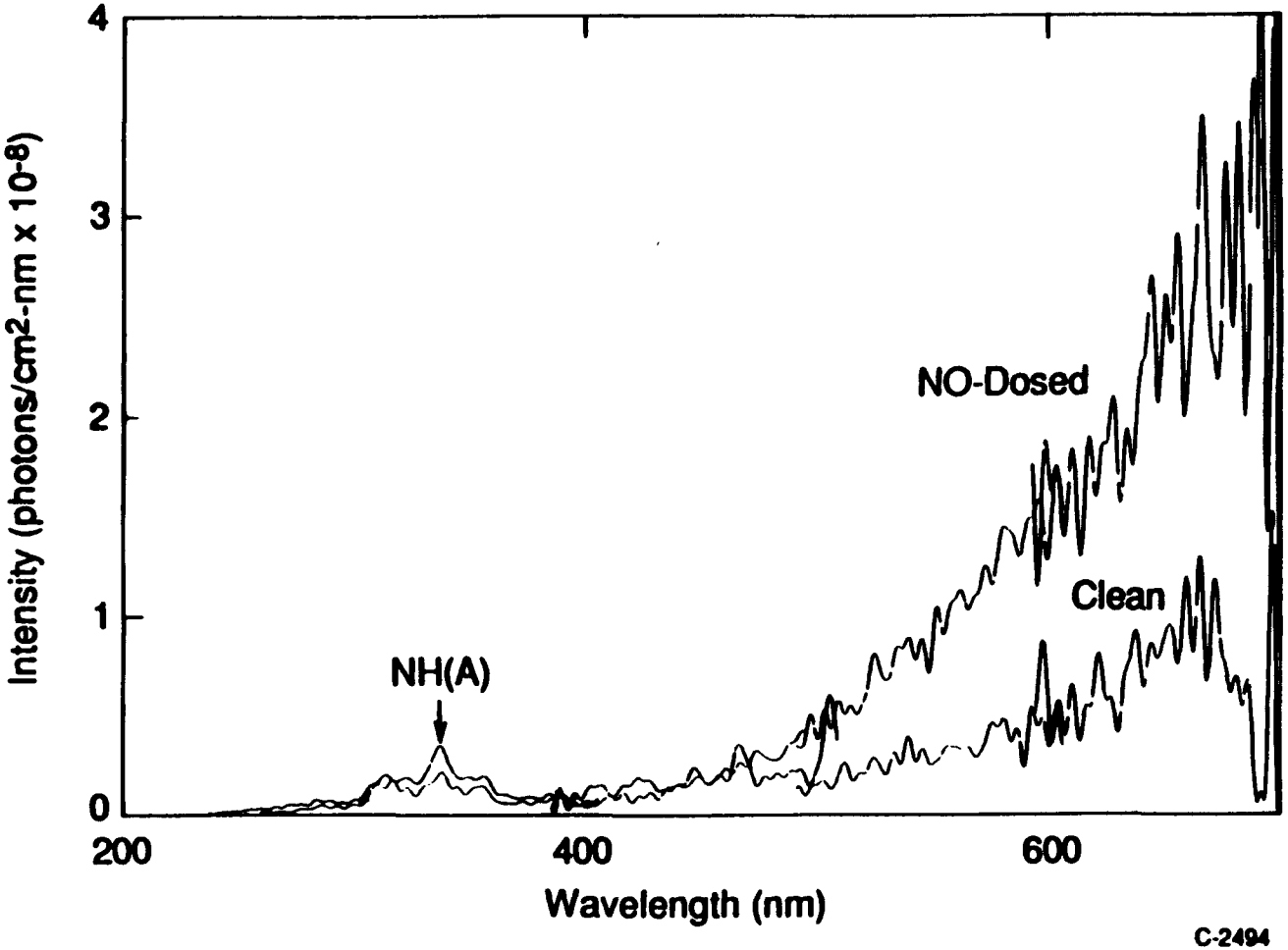

C-2494

OBSERVED ULTRAVIOLET SIGNATURES CU SURFACE, O-BEAM, 8 km/s

T-16440

(Integrated Over 128 Pulses)

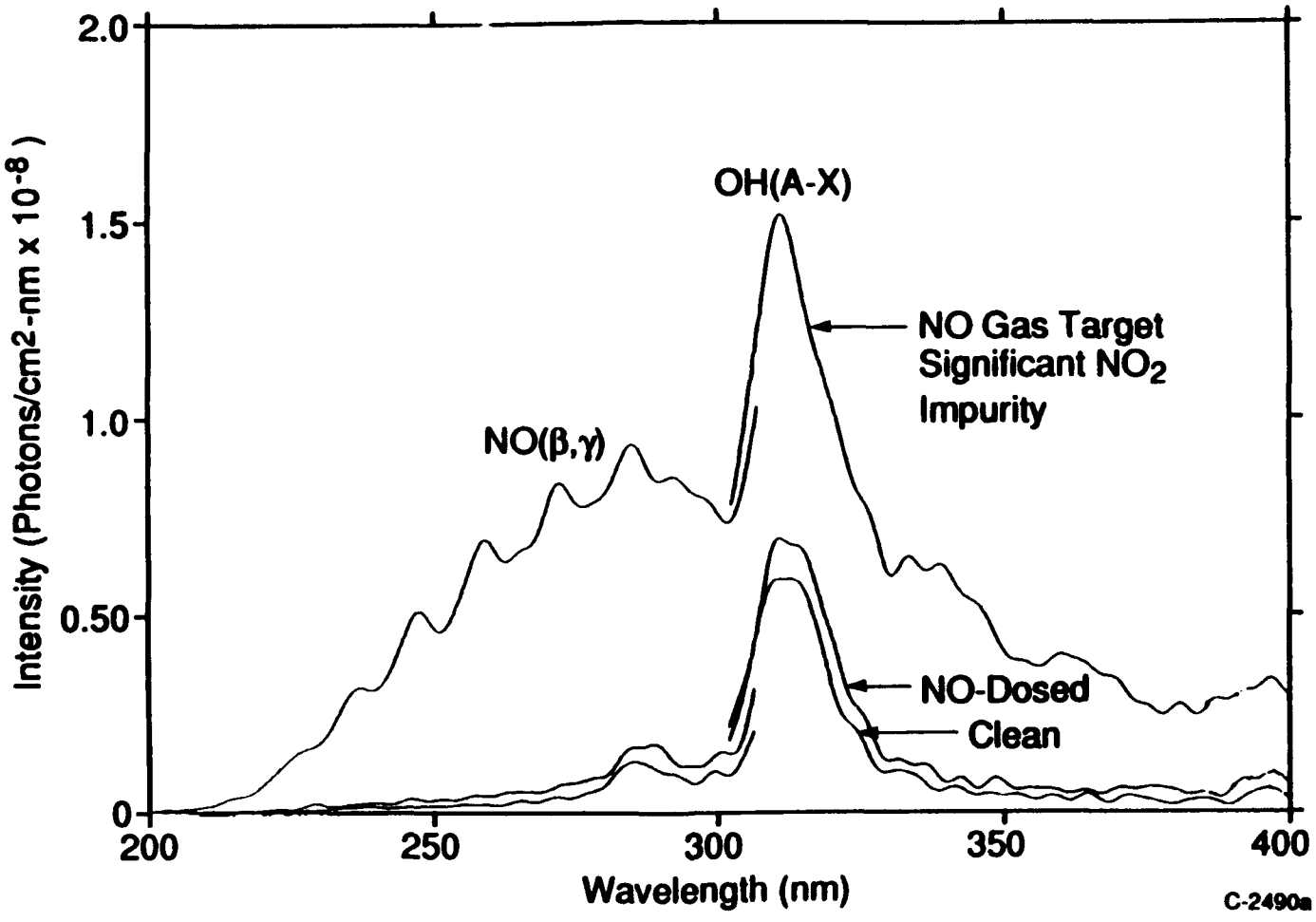

CROSSED BEAM STUDIES OBSERVED GAS PHASE (BEAM/NO) ULTRAVIOLET GLOWS BEAM BACKGROUND SUBTRACTED

T-16441

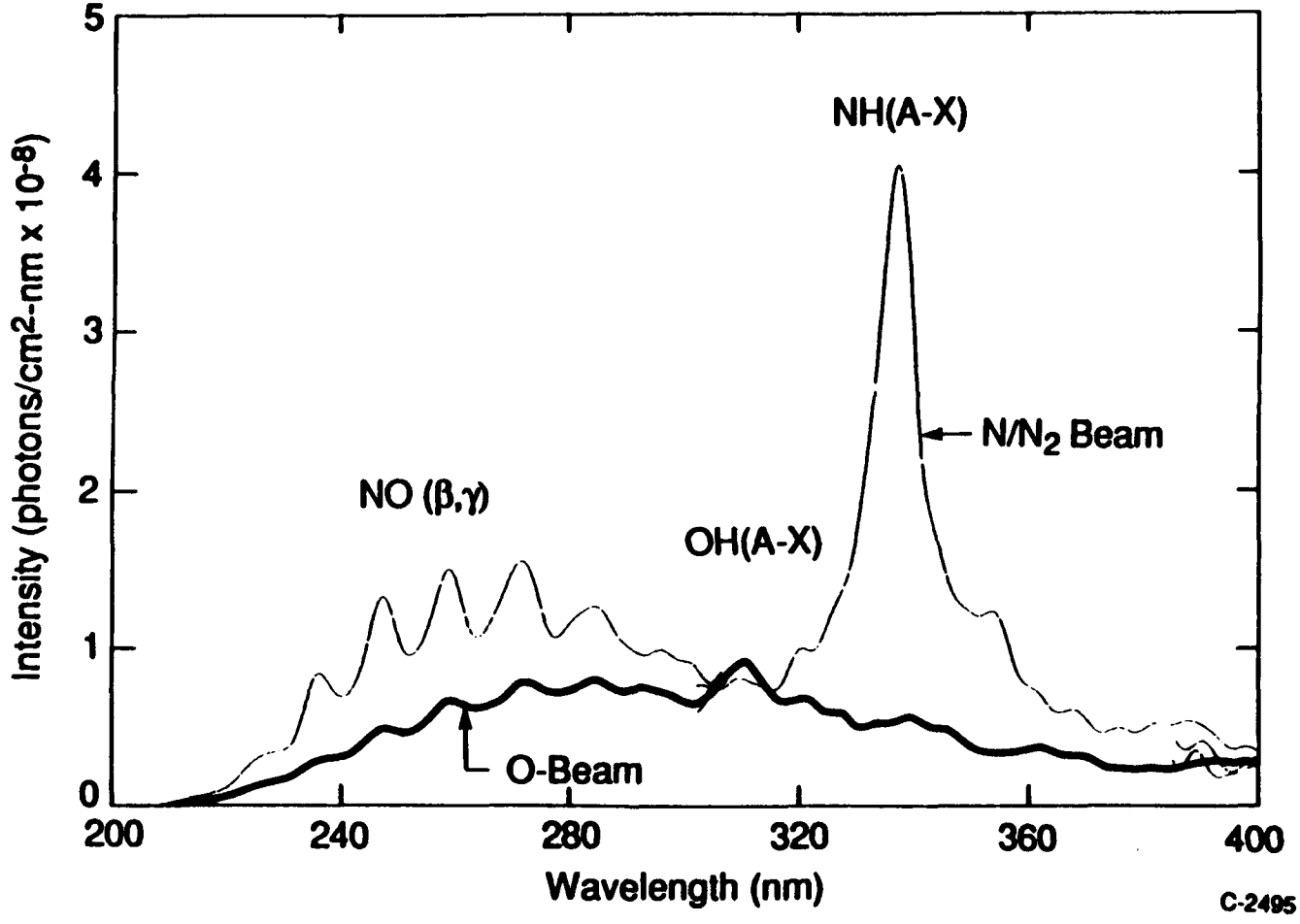

CONCLUSIONS - UV SURFACE AND CROSSED BEAM STUDIES

T-16442

- In surface studies, UV emissions very small compared to visible emissions
  - — In contrast to Orient et al.; material effects?

- In cross beam studies, two distinct emissions observed
  - — OH(A) (NH(A) for fast N/N beam)
  - — NO/β, γ bands

- Proposed mechanism NO_2^+ recombination (suggested by B. Upschulte)
  - — $O^+, N^+ + NO_2 \rightarrow NO_2^+ + O,N$

    $NO_2^+ + e \rightarrow NO(A,B) + O$

VAE - AE-C,-E GLOW OBSERVATIONS (Yee and Abreu, 1983)

T-16443

Altitude Dependence

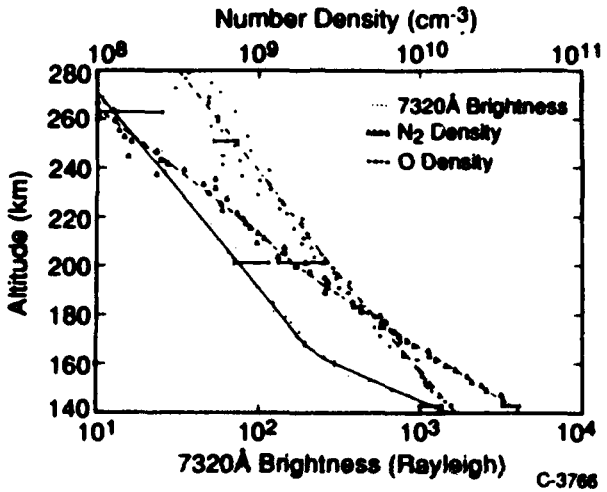

Spectral Variation (GÅ Bandpass Filters)

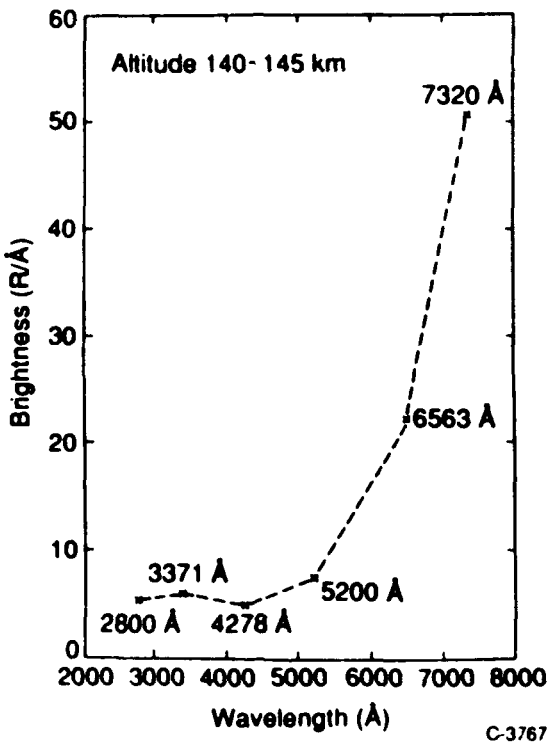

Spectral Variation (GÅ Bandpass Filters)

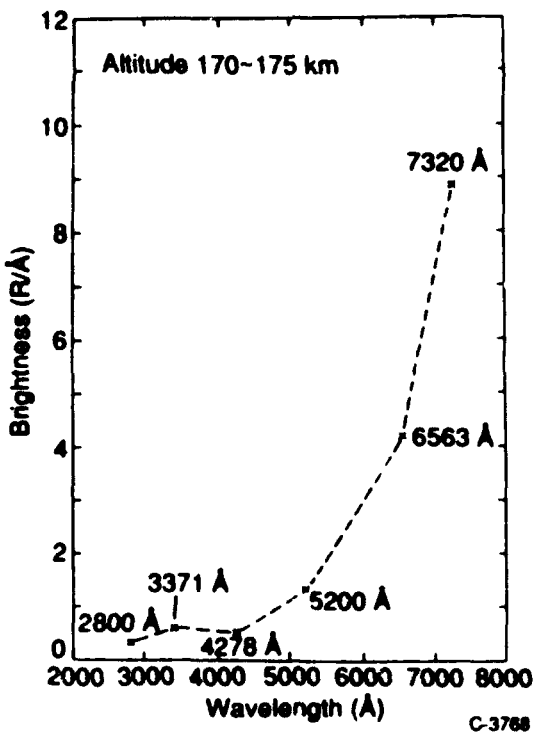

IBSS/AIS OBSERVATION OF UV EMISSION DURING CIV NO RELEASE

T-16444

(SDIO/PL/PSI - Day,Arm)

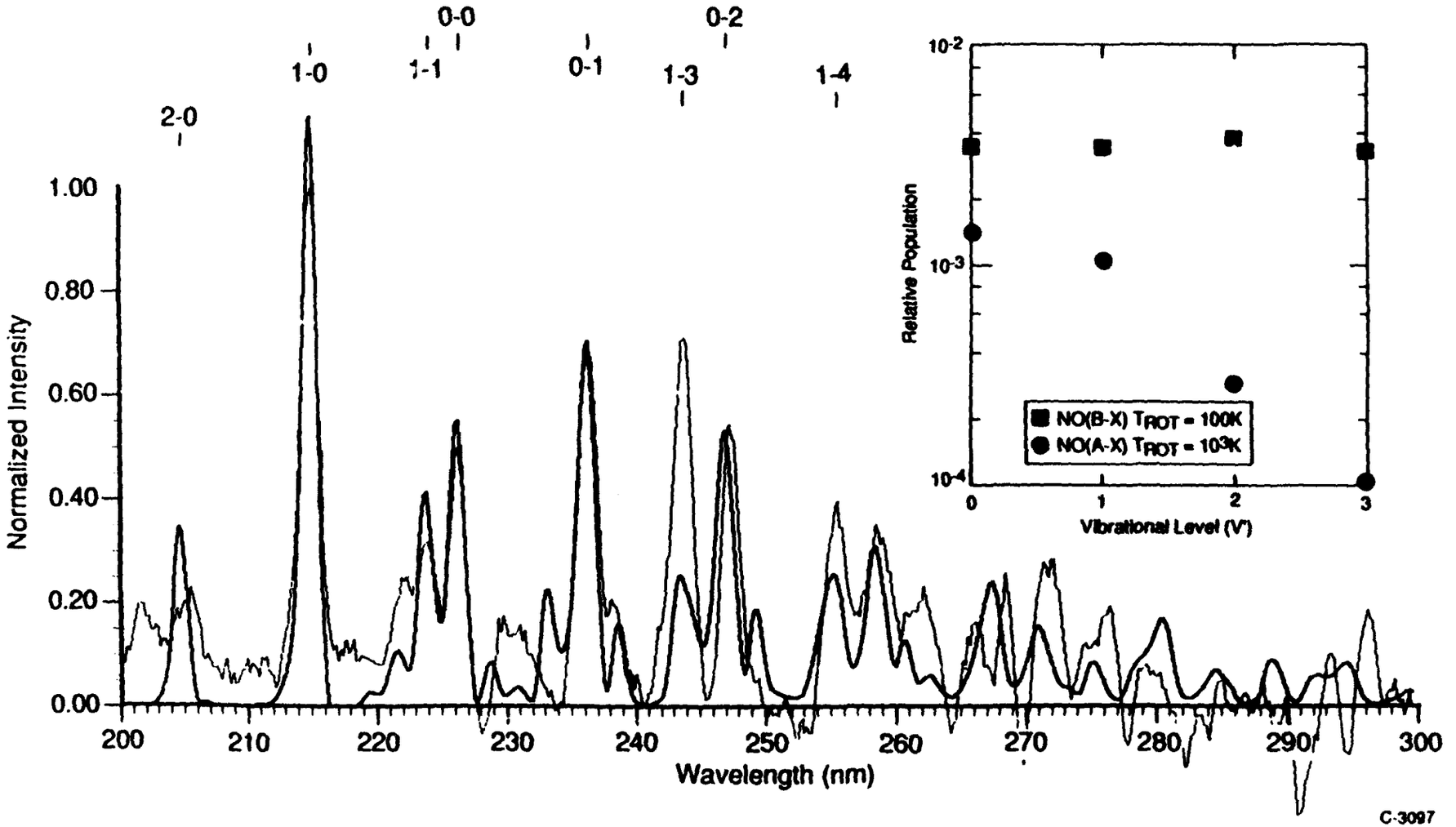

C-3097

VUV GLOWS

T-14645

- Observed by Huffman on S3-4 satellite
- Lyman-Birge Hopfield emission 140 to 170 nm
- Only seen below 230 km
  - — Scales as $(N_2)^3$ or $(N_2)^2(O)$
  - — Suggested source N-atom recombination (Kofsky, Meyerott and Swenson)
  - — No laboratory measurements available

NIGHTGLOW FROM DoD S3-4
Huffman et al., (1980)

T-14646

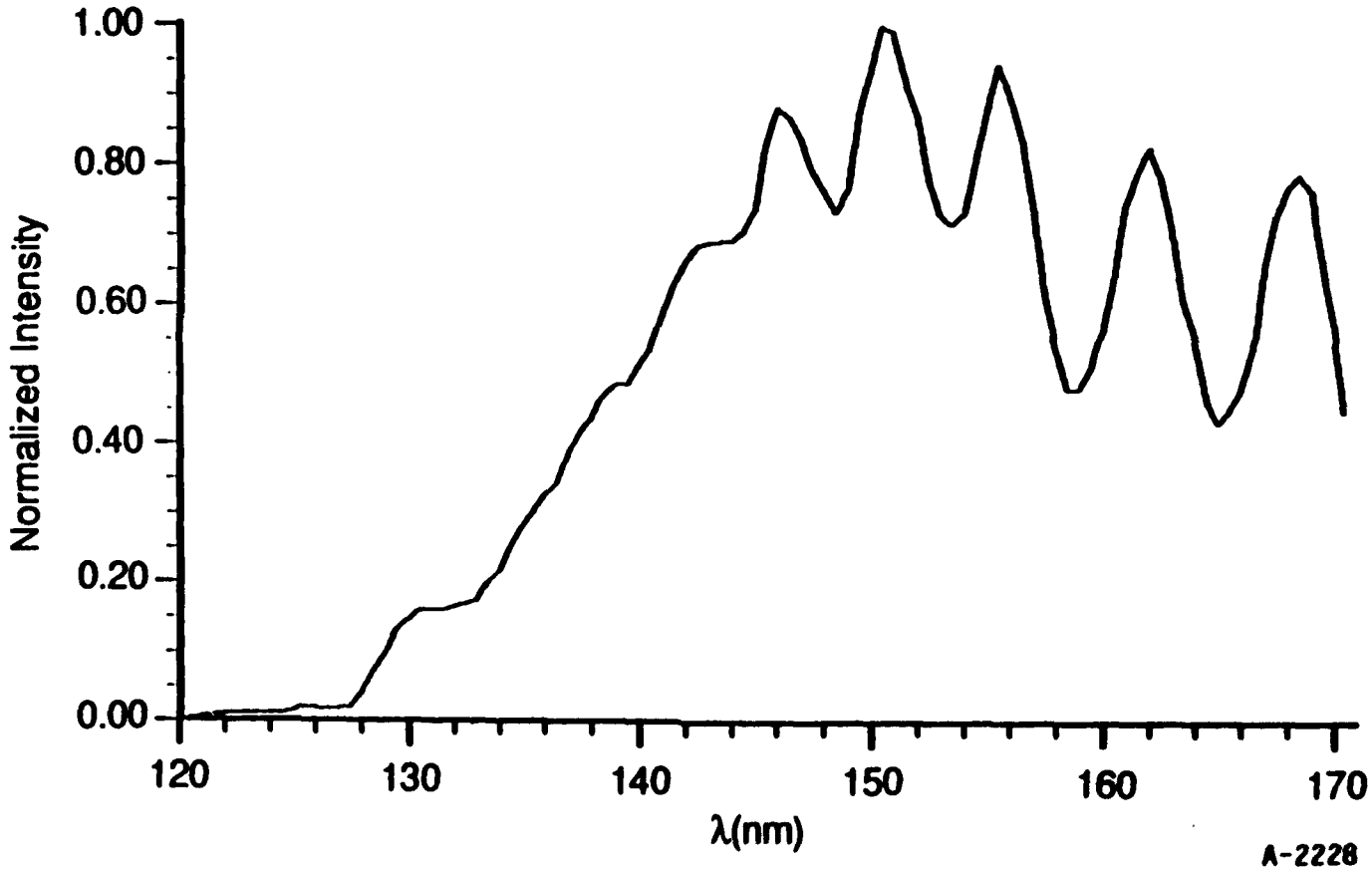

$N_2(a\text{-}X)$ Best Fit (Green)

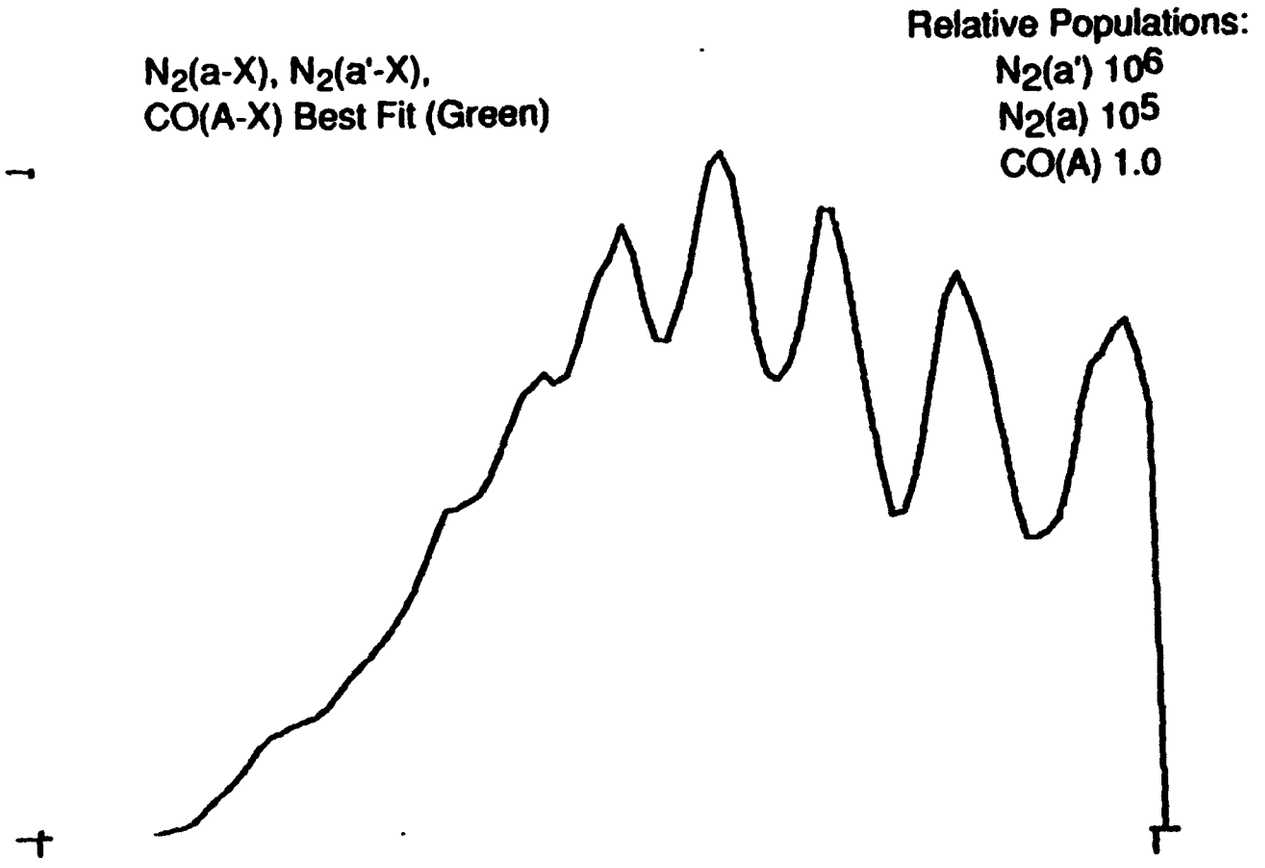
N_2(a-X), N_2(a'-X),
CO(A-X) Best Fit (Green)
Relative Populations:
N_2(a') 10^6
N_2(a) 10^5
CO(A) 1.0

SUMMARY

T-16445

- A surface glow for every occasion
- Accommodation behavior critical in specifying surface glow intensities
  - — Material dependent
  - — Temperature dependent
- Anticipate that different mechanisms will come in play with changing trajectory altitude